MASTER DRAFT

Chapter #10:
PARTICLE LIFTING PROCESSES IN DUST DEVILS

Authors: L.D.V. Neakrase[1], M.R. Balme[2], F. Esposito[3],T. Kelling[4], M. Klose[7,10], J.F. Kok[6], B. Marticorena[5], J. Merrison[8], M. Patel[2,9], G. Wurm[4]

[1] Department of Astronomy, New Mexico State University, Las Cruces, NM, USA.
[2] Open University, Walton Hall, Milton Keynes, MK7 6AA, UK.
[3] INAF – Osservatorio Astronomico di Capodimonte, Napoli, Italy
[4] Faculty of Physics, University of Duisburg-Essen, Duisburg, Germany
[5] Laboratoire Interuniversitaire des Systèmes Atmosphériques, Université Paris – Créteil, France
[6] Department of Atmospheric and Oceanic Sciences, UCLA, Los Angeles, CA, USA
[7] Institute for Geophysics and Meteorology, University of Cologne, Cologne, Germany
[8] Institute of Physics and Astronomy, Aarhus University, Aarhus, Denmark
[9] Space Physics, Rutherford Appleton Laboratory, Oxfordshire, UK.
[10] USDA-ARS Jornada Experimental Range, Las Cruces, NM, USA

Abstract
Particle lifting in dust devils on both Earth and Mars has been studied from many different perspectives, including how dust devils could influence the dust cycles of both planets. Here we review our current understanding of particle entrainment by dust devils examining results from field observations on Earth and Mars, laboratory experiments (at terrestrial ambient and Mars-analog conditions), and analytical modeling. Interactions across these three fields provides a unique perspective for examining interactions between particle lifting processes from mechanical, thermal, electrodynamic and pressure effects, and how these processes apply to dust devils on Earth and Mars. We examine how differences in particle lifting processes affect dust devil sediment entrainment on these planets.

1.0 Introduction

Dust devils are vertical convective vortices that are intense enough to erode surficial particulate materials and perhaps even weakly-indurated sediments. They are of scientific interest because of their potential to lift considerable amounts of surface material into the atmosphere. In contrast to regular boundary layer winds, dust particles (D_p < 63 μm) are more easily removed from the surface by dust devil action than by boundary-layer wind shear alone (Greeley et al., 2003). This has been proposed to be due to a combination of influences dubbed the *"∆P-effect*" by Greeley et al. (2003), in reference to the idea that the low–pressure core of a dust devil might "suck-up" material.

Understanding this effect is important for Mars because of the many dust devils seen there (e.g., Metzger et al., 1999; Cantor et al., 2006; Greeley et al., 2006; 2010), and the likelihood that the low atmospheric density means that small particles are difficult to lift by boundary layer winds alone (Greeley and Iversen, 1985). The dust cycle on Mars (Kahn et al., 1992; Zurek and Martin, 1993; McKim, 1996; Newman et al., 2002) dominates much of the weather on Mars, and has many sources and sinks responsible for regulating the global movement of fine-grained material. The martian dust cycle includes interactions between multiple drivers of dust entrainment, such as dust storms, dust devils, polar outflow, and dust removal processes – dominantly, dust settling out from the atmosphere over time. Dust devils and dust storms are the major contributing sources for atmospheric dust on Mars (e.g., Newman et al., 2002; Kahre et al., 2006). Beyond understanding the nature of martian weather, the dust cycle plays an integral role in the continued exploration of Mars: dust constantly settles out of the atmosphere onto spacecraft sent to Mars to explore the surface, affecting surface mobility and power generation (Greeley et al., 2006, 2010). It is possible that the electrostatic properties of fine grains can wreak havoc with moving parts. However, the enhanced ability of dust devils to lift fine grains provides a beneficial effect: sometimes removing dust from spacecraft solar panels as the dust devils pass over them (Greeley et al, 2006, 2010; Lorenz and Reiss, 2015).

Dust devils, although localized, small-scale meteorological phenomena, seem to be more significant sources of atmospheric aerosols on Mars than on Earth (e.g., Metzger et al., 1999; Balme and Greeley, 2006; Greeley et al., 2010; Allen et al., 2015; Jemmett-Smith et al., 2015, see also Klose et al. *this issue*). The presence of dust devils on Mars has led to many dust devil laboratory and field studies aimed at investigating their ability to lift fine particles, which explore the idea that dust devils might be

the cause of pervasive background dust loading required to maintain the ongoing dustiness of the martian atmosphere (Montabone et al., 2015). Exactly how dust devils lift fine-grained sand and dust is not well understood, being a complex set of interactions within a transient, micrometeorological process. However, significant work has been performed to investigate the conditions responsible for the enhanced lifting capabilities of dust devils compared to simple boundary layer flow.

On Earth, dust devils share many attributes of their martian counterparts, but are smaller in size, perhaps due to Earth's shallower planetary boundary layer. Dust devils occur frequently in arid and semi-arid regions of the Earth, where sensible heat fluxes are large, and loose sediment is available (e.g. Sinclair, 1969; Snow and McClelland, 1990; Hess and Spillane, 1990; Oke et al., 2007; Kurgansky et al., 2011; Lorenz et al., 2015). They rarely form in other regions, where aeolian sediment transport is severely hampered by the presence of soil moisture or vegetation, which reduce sensible heat fluxes and prevent the lifting of soil particles. Due to their localized impact, less attention has been paid to dust devils in dust modelling than to regional or even continental-scale dust storms (see Chapter 11). In addition, turbulence in the atmospheric boundary layer is highly stochastic and, although bulk properties are relatively well understood (e.g., Kaimal and Finnigan, 1994; Smits et al., 2011), the explicit prediction of sub-gridscale phenomena such as dust devils remain difficult to represent in atmospheric circulation models.

In this paper, we aim to review our current understanding of the processes involved in dust devil sediment lifting, including a discussion of possible contributing factors to the "ΔP-effect". After reviewing the general physics of aeolian particle lifting (Section 2), we discuss insights into particle lifting specifically by dust devils with respect to: (i) results from Mars and Earth field observations (Section 3.1), (ii) laboratory experiments (Section 3.2), and (iii) analytical modeling (Section 3.3). Examining all three methodologies together provides a more complete picture of the underlying physics of dust lifting within dust devils, including exploring why all thermal vertical vortices are not necessarily capable of lifting dust, and what the dust lifting potential on Earth and Mars implies for the global and regional dust budgets of both planets.

2.0 Physics of Particle Lifting

There is a long history of the study of aeolian particle movement which dates back to the early 20th century, including wind tunnel experiments and observations pertaining to the movement of sand in dunes and ripples (Bagnold, 1941; Chepil, 1945). Observations showed that aeolian sediment transport is initiated if the atmospheric aerodynamic momentum fluxes (expressed in terms of a friction velocity, u_*) exceed a threshold value (threshold friction velocity, u_{*t}). This value, u_{*t}, is a property of the surface, describing its resistance to wind erosion (Shao and Lu, 2000). Theoretical considerations on the balance of forces acting on a particle at rest lead to estimates on u_{*t}. By accounting for aerodynamic drag and gravity forces, Bagnold (1941) obtained

$$u_{*t} = A_B(Re_{*t})(\sigma_p g d)^{1/2} \quad (1)$$

where σ_p is the ratio of particle to air density ratio, g is the gravitational acceleration, d is the particle diameter, and the coefficient A_B is a coefficient that depends on the particle friction Reynolds number, Re_{*t}. According to Equation (1), u_{*t} increases monotonically with particle diameter. However, observations have shown that there exists a minimum of u_{*t} for particles with diameters of ~100 µm, with u_{*t} increasing with decreasing particle size below that value (e.g. Iversen et al., 1976) (Figure 1a). By further including aerodynamic lift and interparticle cohesion in addition to drag and gravity, u_{*t} including this minimum can be predicted (Iversen and White, 1982; Greeley and Iversen, 1985)

$$u_{*t} = A_1 F(Re_{*t}) G(d) \quad (2)$$

where A_1 is an empirical constant and F and G are relatively complex empirical functions. Shao and Lu (2000) found that these functions can be replaced by a simple theory-based expression if interparticle cohesion is treated explicitly, and if the Reynolds number dependence of aerodynamic forces is neglected. They obtained:

$$u_{*t} = A_N(\sigma_d g d + \gamma/\rho d)^{1/2} \quad (3)$$

where A_N is a dimensionless coefficient, and γ [N/m] scales the interparticle force.

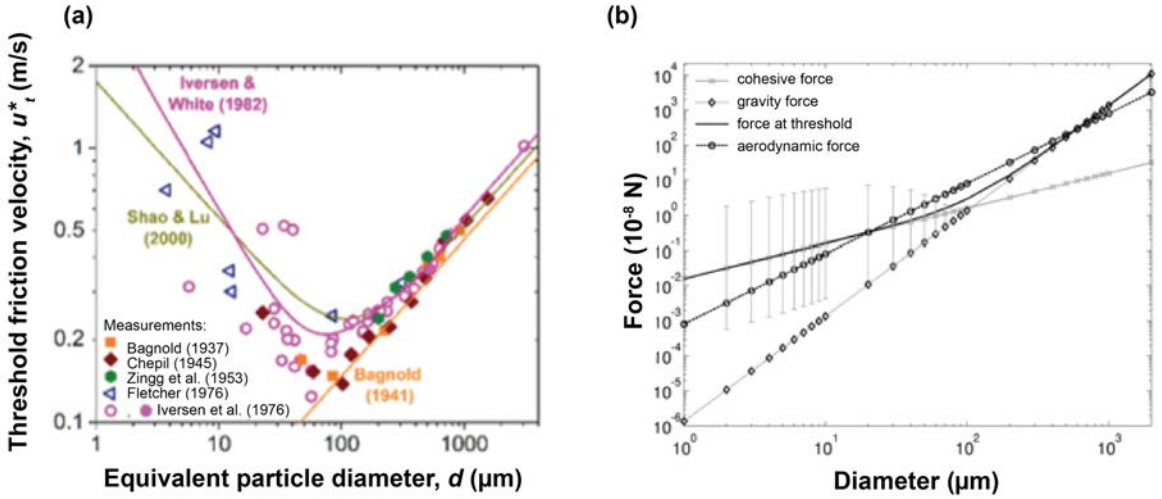

Figure 1: (a) Theoretical relations for the threshold friction velocity from Bagnold (1941), Greeley and Iversen (1985) and Shao and Lu (2000) (colored lines), with experimental measurements using sand and dust (filled symbols) and other materials (open symbols). After Kok et al. (2012). (b) Relative importance of forces relevant for dust emission (from Klose (2014), modified from Shao (2008)). The aerodynamic force is shown for $u_* = 0.4$ m s^{-1}. Error bars indicate the standard deviation of the cohesive force as given in Klose et al. (2014, Eq.8). The stochastic nature of the cohesive force may lead to particle uplift at a lower threshold.

If roughness elements on the soil surface are present or if the soil is moist, the shear stress required to mobilize particles is larger than predicted based on u_{*t} for idealized (smooth and dry) surfaces. Drag partition is used to describe the influence of roughness elements on the surface momentum flux. In drag partition, the total drag is decomposed into a pressure drag on the roughness elements, a drag on the roughness element surface, and a drag on the ground surface (e.g. Schlichting, 1936; Arya, 1975, Raupach, 1992; Raupach et al., 1993; Marticorena and Bergametti, 1995, Shao and Yang, 2008). The fraction of surface to total drag is then used to correct u_{*t} (Marticorena and Bergametti, 1995, Marticorena et al., 1997; Shao, 2008), or the wind stress exerted on the bare soil (Kok et al., 2014b). For Earth, the moisture cohesion must be additionally accounted for in parameterizations of u_{*t}. Parameterizations for this effect have been developed by McKenna-Neuman and Nickling (1989), Fecan et al. (1999), McKenna-Neuman et al. (2003), and Cornelis et al. (2004a, 2004b).

Due to the minimum in u_{*t}, sand particles or particle aggregates with diameters ~100 μm are most readily entrained aerodynamically. Corresponding to their large sizes, such grains are often too heavy to remain suspended. Rather, they hop along the surface horizontally in a process called saltation. During saltation, dust can be emitted either by the impacts of saltating particles overcoming the energetic interparticle bonds between soil particles, which is called saltation bombardment or sandblasting (Gillette, 1974; Shao et al., 1993), or by the physical break-up of saltating dust aggregates transported in saltation (Shao, 2001; Kok et al., 2014b) (Section 2.3).

Dust particles generally need stronger aerodynamic forces for direct aerodynamic entrainment than sand-sized particles, due to the larger entrainment thresholds (Figure 1). Since particle weight scales with d^3, whereas most cohesion forces are thought to scale with d (Hamaker, 1937; Johnson et al., 1971), the interparticle cohesion force f_i is the dominant retarding force acting on small particles. Interparticle cohesive forces include Van der Waals forces, electrodynamic forces, and chemical forces (e.g., Castellanos, 2005). These are governed in turn by a variety of factors such as particle shape, particle surface roughness, and chemical composition. Although theory suggests that f_i is, on average, proportional to d (Hamaker, 1937; Johnson et al., 1971), the influencing factors suggest a stochastic behavior as has been observed by Zimon (1982). This stochastic behavior is more relevant for dust-sized particles than for sand-sized particles, as for the latter, gravity dominates the retarding forces and interparticle cohesion is small in comparison (Figure 1b). The lifting of dust-sized particles is thus also possible through direct aerodynamic entrainment and without saltation as an intermediate process (e.g. Loosmore and Hunt, 2000; Roney and White, 2004; Macpherson et al., 2008; Chkhetiani et al., 2012; Klose et al., 2014). Although the flux of directly entrained dust is typically smaller (for most natural surface types) than the dust amount lifted by the much more efficient saltation-bombardment mechanism, it can become a dominant mechanism in the absence of saltation, i.e. if $u_* < u_{*t}$. For

example, while mean wind shear stresses may be below u_{*t} during a calm summer day, organized atmospheric turbulence can produce shear stresses strong enough to aerodynamically lift dust particles (Klose and Shao, 2013). This is especially the case for dust devils due to intense shear stresses associated with their rotation (e.g. Balme et al., 2003). Additionally, turbulent shear stresses can generate intermittent saltation leading to further dust emissions (Stout and Zobeck, 1997; Dupont et al., 2013).

3. Dust devil sediment entrainment

Dust devils contain complicated wind fields that include significant rotational components, near-surface inflows, and vertical up and downdrafts within the core. In addition, many dust devils vary rapidly in intensity, and even when the dust devil as a whole is in a steady state, the wind field can change significantly at the small-scale as the vortex traverses the surface. Nevertheless, by using a combination of approaches, there has been significant progress in understanding how, and how much, material is lifted by dust devils.

Dust devils may contain a variety of structural and morphological features including all or some of the following depending on the ambient conditions, as well as on the internal pressure structure. Visualization of each of these conditions is dependent on the availability of sediment to trace the dust devil's helical flow. The most dramatic feature of a fully developed dust devil is the dust column (Fig. 2, number 1), which comprises dust lofted from the surface wrapped up around a central thermal updraft. Dust is lifted by a combination of the shear stress from air inflow at the base of the dust devil and other, poorly understood mechanisms, such as low-pressure core effects, popping individual dust grains and/or aggregates of dust into the helical flow (Sinclair, 1966; Balme and Greeley, 2006; Balme and Hagermann, 2006). The column's full extent is highly dependent on the ambient conditions and the strength of the vortex itself. In many weak cases, dust devils may only produce a partial column due to inadequate flow velocities, small core pressure gradients, or sediment availability.

Another common feature in many dust devils is a saltation skirt. Saltation skirts (Fig.2, number 2) can be seen around the base of a dust devil demarking sediment load initially lofted by the dust devil but comprised of particles that are too large or heavy to be suspended in the column. The presence of this saltation skirt is highly dependent on the particle size distributions at the surface and the strength of individual dust devils (Balme and Greeley, 2006). In some cases the larger grains in the saltation skirts can be thrown out of the skirt producing a cycloidal deposition track as is often seen on Mars and rarely on Earth (Greeley et al., 2004; Neakrase, 2009; Reiss et al, 2010; Neakrase et al., 2012).

In many of the strongest dust devils, a clear central core may be observed (Fig.2, number 3). This feature requires a strong pressure gradient within the dust devil allowing a central, dust-free, downdraft to form (Sinclair, 1966; Balme and Greeley, 2006). Cooler air in this downdraft is brought into the structure from outside the dust devil at the top: warm, dust-laden air is rising and rotating upwards around the downdraft.

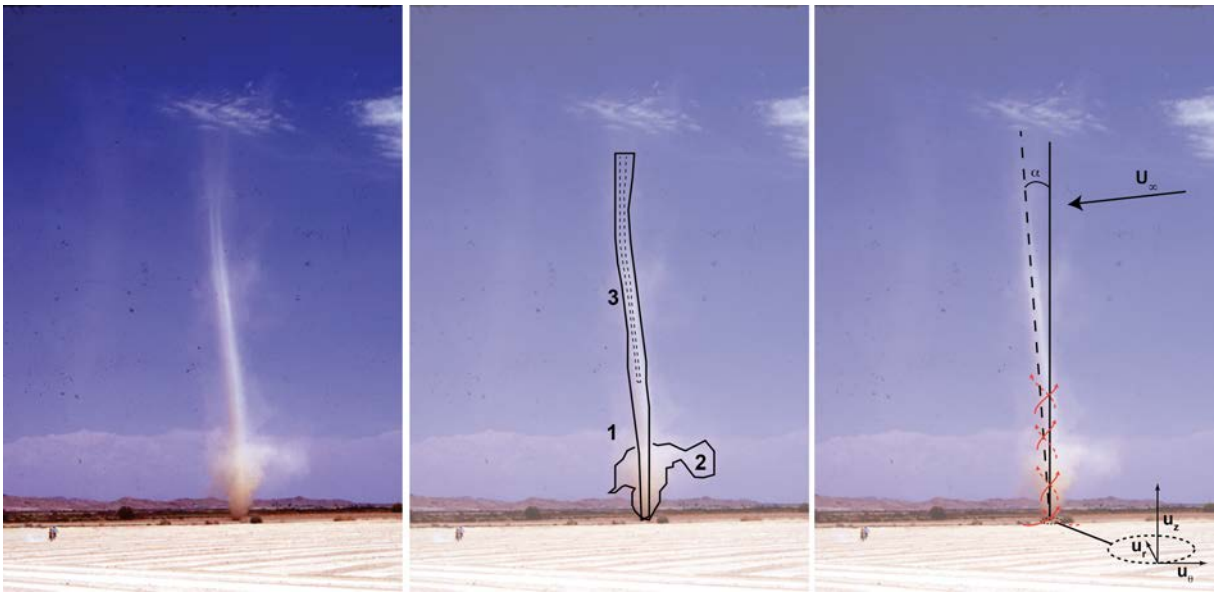

Figure 2. Schematic diagram showing various parts of a dust devil. (Left) 1 represents the main column of the dust devil, 2 shows the "saltation skirt" where larger and heavier particles fall out of the column, and 3 where there are sometimes dust-free core downdrafts. (Right) Shows the individual velocity components of dust devil vortical flow where u_t is the tangential component, u_z, the vertical and u_r, the radial component. U_∞ represents the background boundary layer wind that tilts the dust devil column by a proportional angle, α. [Photo credit: S.P. Idso, Arizona, c. 1975]

Once a stable dust devil has formed, it can behave as a single structure. The column can be pushed by the ambient winds, with the ambient wind speed controlling the lateral motion of the dust devil (Balme et al., 2012). Because the ambient boundary layer winds increase with height above the surface, often dust devils will tilt in the direction of motion (Sinclair, 1966; Kaimal and Businger, 1970; Balme and Greeley, 2006). Flow within the dust devil, resulting in a variety of dust devil morphologies, is controlled by complex interactions between all these processes. Figure 3 shows an idealized two-dimensional view of this flow within a dust devil. Stagnation points where flow reverses within the dust devil can occur near the surface, where the strength of the updraft can allow a region of no flow near the center. If the dust devil is strong enough to have a clear core, another stagnation point can form at the interface of where the downdraft meets the rising, warm, dust-laden air.

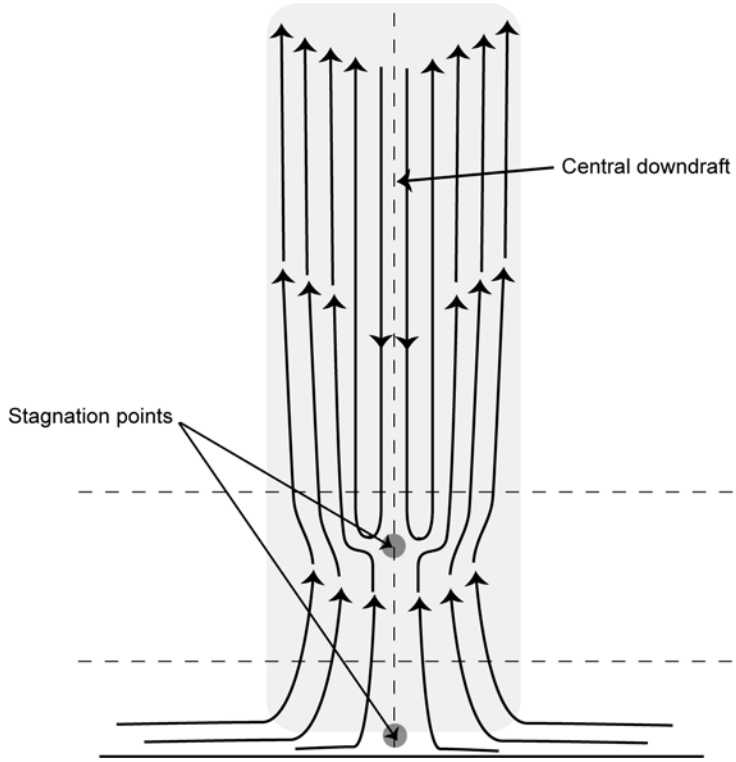

Figure 3. Sketch showing vertical flow within an idealized dust devil. Stagnation points show places where possible flow reversal occurs in some dust devils. The upper stagnation point can be due to the presence of a core downdraft, as observed in some dust devils, and could progress all the way to the surface within the core depending on the strength of the vortex. When an elevated stagnation point is not present, flow within the dust devil is dominated by only vertical flow. (After Balme and Greeley, 2006, and Neakrase, 2009).

3.1 Field Observations

Earth

Various field investigations of dust devils have been made in arid environments on Earth, but only a few have attempted to measure the flux of dust emitted from beneath a dust devil. Renno et al. (2004) used LIDAR to remotely estimate a terrestrial dust devil column peak loading of 100 mg m^{-3} in a dust devil with a peak vertical velocity of 10 m s^{-1} to calculate a dust flux of 1000 mg m^{-2} s^{-1}. The largest data set, though, comes from several field campaigns made between 1996 and 2005 at the El Dorado Playa, Nevada, and near Eloy, Arizona, both USA (Metzger et al., 2011). Metzger et al. (2011) made

measurements using two types of commercial sensor, PM10 (particulate matter with diameter < 10 μm) dust sensors, and TSP (Total Suspended Particle Load) sensors, as well as piezoelectric saltation-impact detectors being tested for the Beagle2 Mars mission (Towner et al., 2004). In many cases, these dust concentration data were acquired at high sample rates allowing particle-load profiles through the dust devil to be made. By combining these data with simultaneously acquired vertical wind speed profile data, they estimated the integrated upwards flux of dust or particulates. Metzger et al. (2014) found that the TSP concentrations in the dust devils they sampled ranged from 6 to 875 mg m^{-3}, whereas the PM10 concentration varied was from 1.3 to 162 mg m^{-3}. From this they extrapolated TSP fluxes of between about 600 to 4375 mg m^{-2} s^{-1} and PM10 fluxes of between 1.3 and 162 mg m^{-2} s^{-1}. Metzger's flux estimates are about an order of magnitude lower than the LIDAR remote sensing ones made by Renno et al., (2004), but this probably reflects the fact that the Metzger data are integrated over profiles of dust load and wind speed, whereas Renno's flux is calculated from peak vertical wind speed multiplied by peak dust concentration. Metzger et al. (2011) also found that the PM10 concentration was around 10% of the TSP value – suggesting that about 90% of sediments entrained by dust devils are too large to be carried into suspension – these forming instead the 'sand-skirt' seen in many dust devils.

While these data can inform about the amount of dust contained in a dust devil, and how rapidly it is lifted, they do not inform about the process by which the dust is entrained. While the ΔP effect could play a role, Balme et al. (2003) showed that the intense winds contained in dust devils generate shear stresses sufficient to lift most natural materials on their own, so it seems likely that, on Earth, shear stress dominates any other effect within dust devils. However, as outlined by Balme and Hagermann (2006), the suction effect created by the low-pressure core of a dust devil passing over a particulate surface is likely to be more effective when particle size is small, and when the dust devil is itself small and travelling quickly across the surface. Hence, there might be occasions, even on Earth, when dust devils can suck material up rather than or in addition to blowing it into motion.

Even on Earth, quantitatively measuring dust vertical lifting is a difficult task and dust emission fluxes data sets are not numerous. A large part of this difficulty comes from the fact that it is difficult to properly sample the large size-range of mineral dust, especially with a high temporal frequency. As a result, most of the available data sets of in situ flux measurements are mass dust emission fluxes measured as a function of the wind friction velocity (Gillette, 1977; Nickling, 1983; Nickling and Gillies, 1993, Nickling et al., 1999; Gomes et al., 2003; Rajot et al., 2003). Dust emission fluxes are usually estimated using the so-called "gradient method". This method is based on the assumption that particles with aerodynamic diameters smaller than 20 μm are light enough to follow air movements perfectly and that the dust flux is constant with height (Gillette et al., 1972). In such conditions the causal relationship of air momentum and particle mass exchanges allows to express the upward vertical flux of particles as a function of the wind friction velocity (u_*) and of the difference of dust concentration measured at two vertical levels (Gillette, 1972). As recently reminded by Shao et al. (2011), even in emission conditions, the diffusive flux is not constant with height due to gravitational settling and a correction may be applied to the computed flux as a function of particle size. For particles in the range of 2 - 3.5 μm, this correction was estimated as being negligible (2%), but it is 15% for particle sizes from 6 to 8 μm, and should be higher for larger particle sizes (Shao et al., 2011).

From field measurements, the computation of u_* is usually performed over durations of 15 min, at least, because this minimal duration is necessary for integrating the major time scales of turbulence occurring in the atmosphere surface boundary layer (Wieringa, 1993). In addition, dust concentration is often measured based on dust collection with filters, which requires a minimal integration time to get measurable dust loads which creates differences in concentration between the different levels of measurements. Dust sampling also involves the use of inlets with a specified size range. The most commonly used is the PM_{10} inlet that allows an efficient collection of particles up to 10 μm. More recently, the gradient method was applied to size-resolved dust measurements performed in Australia (Shao et al., 2009) during the Japanese Australian Dust Experiment (JADE, Ishizuka et al., 2008) and in Niger (Sow et al., 2009), as part of the AMMA (African Monsoon Multidisciplinary Analysis) international project. In both cases, significant vertical dust fluxes were measured only during periods where saltation occurs, confirming the efficiency of the combination of the saltation and sand-blasting processes to produce and release fine dust particles.

Mars

Dust devils were never imaged by the *Viking* landers in the late 1970s but the detection of short isolated pressure drops in the meteorological data (Ryan and Lucich, 1983; Ringrose et al. 2003) suggest that convective vortices (it is not possible to tell whether they were dust loaded or not) did pass over or close to the lander. Further information from these early surface vortex detections was limited due to the low resolution and sampling rate, and the sheltered position of the pressure sensors

on the *Viking* landers. Diurnal and seasonal relationships can be seen as similar to terrestrial cases with peak activity occurring near midday and more detections occurring during the summertime (Ringrose et al., 2003). The signature of the clear core or rather the central downdraft could be seen in the pressure data, but other quantitative information about dust concentration within the column was not available.

Visual surface observations of dust devils began with *Mars Pathfinder* (MPF), in 1997, with the first images of dust devils from a lander. Metzger et al. (1999) discovered dust devils around the lander after employing a filter subtraction method to make the dust devils visible in the enhanced images. They reported the first estimates of dust devil properties, including sizes, speeds, and dust loading made with assumptions based on terrestrial field studies. Assuming vertical velocities of ~7 m s^{-1} and measured dust loading ~70 mg m^{-3}, from MPF dust opacity studies, Metzger et al. (1999) reported calculated estimates of the average dust devil dust flux of ~500 mg m^{-2} s^{-1}. They also estimated a range in dust devil diameter of 14-79 m and estimated heights of 46-350 m. Dust devil traverse speeds were estimated at ~0.5-4.6 m s^{-1}. These represent the first measurements of dust devil properties from the surface of Mars. Ferri et al. (2003) performed a reanalysis of the MPF dust devil data substituting vertical velocities of up to 20 m s^{-1} (based on martian thermal convection studies), and making more detailed estimates of the distances to the dust devils and hence the dust devil diameters. The largest dust devils were determined to be around 100-200 m in diameter with a dust loading of ~700 times the background dust loading. Average dust devil dust fluxes were determined to be ~70 mg m^{-2} s^{-1} for a 200 m dust devil.

Further visual observations during the course of the *Mars Exploration Rover, Spirit* campaign in Gusev Crater (2004-2010) suggested that, as is the case for Earth, dust devil activity and dust lofting capability is highly variable from region to region, and from season to season (Greeley et al., 2006; 2010). Three dust devil seasons were observed from *Spirit* in Gusev Crater, where over 700 individual dust devils were observed. Due to a favorable viewing geometry, namely the location of the rover on the Columbia Hills for each of the dust devil seasons, a more accurate estimate of the distances from the rover to the dust devils was possible. Gusev crater contained relatively few large dust devils – their size ranged from a few meters to upwards of 276 m – but over the three seasons about six dust devils out of 761 were calculated as being larger than 160 m in diameter. Dust fluxes of between 0.004 – 460 mg m^{-2} s^{-1} were estimated, suggesting lower values than the estimates from Ares Valles (MPF), but the frequency of dust devils for Gusev crater was higher during the three seasons (Greeley et al., 2006; 2010) than Ares Valles. The use of higher resolution cameras in conjunction with the better viewing angles is likely the reason so many more smaller dust devils were observed (as many as 51 dust devils per sol) at Gusev compared to Ares Valles. The other improvements used in this mission included “movie” sequences taken by *Spirit*, in which rapidly acquired sequences of images were used to capture dust devil movement. The same dust devil could be captured in many frames in a time sequence. The benefits of these sequences included being able to monitor how dust devils changed with time as they traversed the floor of Gusev Crater and the ability to estimate their translation speeds and hence, indirectly, the instantaneous near-surface wind speeds in the study area. Estimations of vertical velocities were also made within some of the dust devils. Traverse speeds were consistent with 1-3 m s^{-1} ambient winds, and where clumps of sediment could be identified in subsequent frames, vertical velocities were estimated as being between 1-2 m s^{-1} (Greeley et al., 2006; 2010). Other observations from the Mars Exploration Rovers suggest that dust devil induced removal of dust from solar panels occurred, and that this coincided with the peak diurnal dust devil activity when boundary layer winds alone probably would not have been as effective an agent (Greeley et al., 2006; 2010; Lorenz and Reiss, 2015).

During the course of the 2008 Mars Phoenix Lander (PHX) mission several dust devils were detected at high northern latitudes. The meteorological package recorded ~502 pressure drops > 0.3 Pa and lasting at least 20 s, presumably associated with the nearby passage of dust devil-like vortices (Ellehoj et al., 2010). Using a method similar to that used by Murphy and Nelli (2002) to estimate vortex populations at MPF from the meteorological instruments, Ellehoj et al. (2010) examined the frequency of convective vortices at the PHX landing site (68.2°N, 234.3°E).Their results showed that convective vortices at high latitudes on Mars might have complicated initiation mechanisms, including sources of vorticity such as local weather systems and topographic controls. For example, a few vortex signatures were detected at nighttime, when there is no solar input. These nighttime vortices are hypothesized to be due to vortex shedding from surrounding topographic features. Vortex detections at the PHX site peaked with the typical midday activity for dust devil populations, albeit having a slightly earlier peak than previously measured on Mars, but the seasonal activity was different due to the high latitude and interactions with weak frontal systems and topographic controls (Ellehoj et al.,

2010). Measured ambient winds during the PHX mission were on average 4-5 ms^{-1} in the NE-SE direction with estimated vortex wind speeds of 5-10 m s^{-1} (Ellehoj et al., 2010; Holstein-Rathlou et al., 2010), well below the boundary layer wind tunnel estimates of ~30 ms necessary for dust entrainment (e.g., Greeley and Iversen, 1985) but similar to values obtained from other landing sites.

Surface observations of martian dust devils have all suffered from the same issues that hinder good correlative studies: firstly, visual detections of dust devils (e.g., Greeley et al., 2010) are generally not available with correlated meteorological information (i.e., pressure, temperature, wind speed, etc.). Secondly, meteorological detections of convective vortices, as in the *Viking*, *Pathfinder*, and *Phoenix* cases, generally lack simultaneous images. This dichotomy illustrates the difficulties in documenting such a transient natural phenomenon, compounded by remote sensing limitations of exploring a planet other than Earth.

3.2 Laboratory Investigations

3.2.1 Mechanical studies & the Arizona State University Vortex Generator (ASUVG)

Terrestrial boundary layer wind tunnel studies of sediment lifting have shown repeatedly that threshold curves for different particle sizes and densities, and different ambient pressures (Bagnold, 1941; White et al., 1983/84; reviewed in Greeley and Iversen, 1985, etc.) could be extrapolated to other planetary bodies with similar results. Namely higher threshold wind speeds are needed for lifting smaller particles in the same way that stronger winds are needed to lift larger particles.

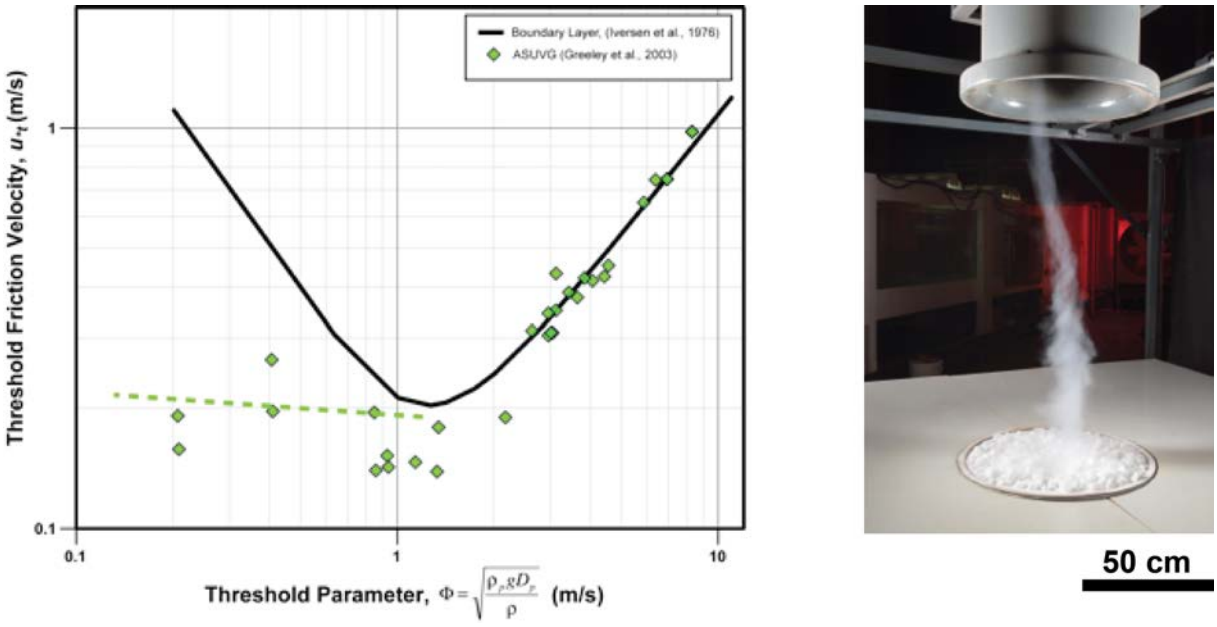

Figure 3. Plot of the threshold parameter (left), Φ, versus threshold friction speed, u_{*t}, showing differences in laboratory data comparing boundary layer versus vortex induced particle thresholds, where ρ_p is particle density, g is gravity, D_p is particle diameter, ρ is atmospheric density. Image of the ASUVG with CO_2 sublimate for flow visualization (right). (After Greeley et al., 2003, and Neakrase and Greeley 2010a)

Laboratory studies of the mechanical properties of dust devils were conducted via a series of experiments using the Arizona State University Vortex Generator (ASUVG) (Greeley et al., 2003; Greeley et al., 2005; Neakrase et al., 2006, Neakrase and Greeley, 2010a; 2010b). These experiments explored dust devil sediment flux and basic interactions with surface roughness. Initial threshold studies (Greeley et al., 2003) demonstrated that vortices were very efficient at lifting small particles (Figure 3), suggesting that a rotationally induced pressure drop in the core of the vortex was providing an additional lift component that was substantial enough to overcome the interparticle forces acting on the small grains and hence allowing them to be more easily lifted into the dust devil column.

Further laboratory characterization of this "ΔP-*effect*" examined sediment flux for vortex flow on both aerodynamically smooth and rough surfaces (Neakrase et al., 2006; Neakrase and Greeley, 2010a;

2010b). Expanding on the threshold experiments of Greeley et al. (2003), sediment flux was examined for a variety of materials at a range of tangential velocities (1-45 ms^{-1}), which were above the measured threshold for both terrestrial ambient and martian analog conditions. The parameterized sediment flux was demonstrated to be a function of the strength of the vortex, described by the 'lifting parameter', $\Delta P/u_*$. The use of this parameter allowed comparison in both Earth and Mars environments, and accommodated the non-coupled nature of the core pressure differential and the tangential velocity. In other words, the tangential velocity is not determined solely by the size of the vortex, meaning that for the same sized vortex, there could exist multiple configurations of ΔP and tangential velocity (Neakrase et al., 2006; Neakrase and Greeley, 2010a). The empirical results of their work showed dust devil sediment flux is proportional to the lifting parameter to the fourth power.

Balme and Hagermann (2006) also sought to examine the nature of the "ΔP-*effect*" by using two different simple numerical models to explore how vertical pressure gradients (caused by, for example, the passage over the surface by the low-pressure core of a dust devil) might lift loose particles. The two competing mechanisms described by Balme and Hagermann (2006) included 1) an impermeable bed of particles with lifting by vertical pressure gradients only, and 2) a bed in which lifting is controlled by the drag forces on particles as gas is sucked out from the interparticle pore spaces. Their conclusion was that the vertical pressure-gradient process alone was the more efficient and effective process, suggesting that equilibration of pore space pressures with the transient passage of the localized low-pressure system led to a decrease in the lifting potential of the vortex. Hence, pressure-gradient lifting would be most effective when the pressure gradient is applied suddenly, and when the particles size of the sediments is small, such that 'degassing' from the interparticle pore-spaces happens slowly compared to the application of the pressure gradient. Hence, the ΔP effect would be most effective in small, fast-moving (across the surface) dust devils with intense low-pressure cores. This might explain why the ΔP effect was seen so clearly in the small, laboratory-scale vortices, but is yet to be seen in the natural dust devil size regime. It is possible that this effect is negligible in real dust devils.

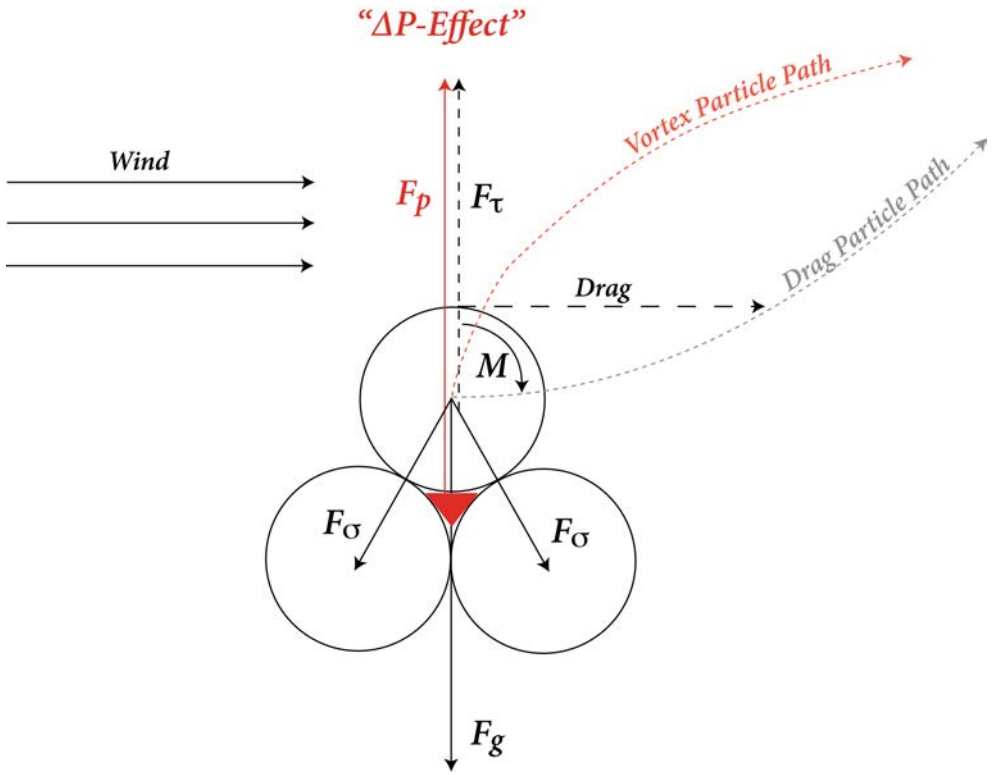

Figure 4. Simplified force diagram showing idealized forces acting on a particle as it is lifted in boundary layer flow (gray) and vortex flow with ΔP-effect (red). F_g represents gravity, F_σ, interparticle forces, M, the Magnus rotational force, F_τ, the lift component from boundary layer shear stress, and F_p, lift component from the change in pressure possibly resulting from pore space pressure equalization. (After Greeley et al. (2003), Neakrase and Greeley (2010a), and Balme and Hagermann (2009)).

Other experiments in Mars simulation wind tunnels demonstrate fine dust (<10μm) entrainment (re-suspension) occurs at surface shear stress of order 0.01 Pa (corresponding to wind speed <15 m s^{-1}) (e.g., reviewed in Greeley and Iversen, 1985) This is in good agreement with wind speeds observed (measured) at the surface of Mars during dust entrainment (including dust devil like events). This threshold value also agrees reasonably with the threshold surface shear used in global circulation models for Mars (Newman et al., 2005; Rathlou-Holstein et al. 2010). According to models based upon direct entrainment of sand (Shao and Lu 2000), dust should require shear stress an order of magnitude higher than these values.

One possible explanation presented and discussed in the 1970s (e.g., reviewed in Greeley and Iversen 1985), was that aggregated dust could be removed as 'low density sand particles'. In support of this claim dust aggregates are seen to be ubiquitous on Mars (e.g., Sullivan et al. 2008). Experiments in wind tunnels have also recently demonstrated that the threshold wind speed (and rate) falls significantly for increased deposited dust depth (i.e., greater than 1 mono layer) supporting the idea that when dust can form aggregates, it is easier to lift (Rondeau 2015, Merrison et al. 2007, Merrison et al. 2012). The detailed micro-scale dynamics of aggregate removal/breakup has yet to be studied in detail, however the experimental techniques necessary for such studies (e.g., the use of high-speed cameras or laser-based velocimetry) are readily available.

It is widely accepted that the simple boundary layer model typically used in sand/dust entrainment is incomplete and that in most cases turbulence plays a significant role in aeolian mobilization (Ibrahim et al. 2008, Reeks and Hall 2001, Ziskind et al. 1995, Dupont et al., 2013, Klose et al., 2014, Carneiro et al., 2015). The role of turbulence has been widely discussed in experiments and modelling of dust (and sand) entrainment, though there has been limited success in implementing a quantitative model to reproduce observed dust re-suspension (e.g., Rondeau et al. 2015).

It is typical in wind tunnel studies of sand transport that mobilization (detachment) occurs at significantly lower wind speeds (shear stress) than entrainment (lift). This type of transport, thought to result from rolling detachment, is a pre-cursor to entrainment. It has been shown that rolling detachment can have a qualitatively different behavior than the conventional aerodynamic model (e.g., De Vet et al. 2014, Reeks and Hall 2001), and could lead to particles on Mars being lifted by winds at speeds below the usually considered aerodynamic threshold.

In summary, although wind tunnel and vortex generator studies have demonstrated that small vortices are particularly efficient at lifting particles of all sizes under both terrestrial and martian conditions, they have not been able to explain the process by which this occurs specifically. As wind tunnel studies progress, there has been new recognition of the effects of saltation triggering, rolling and turbulence on the lifting of dust and sand. All of these mechanisms are probably important for dust devils on Mars, but, as shown below, other, perhaps less intuitive, effects might also play a role.

3.2.2 Thermal lifting

It is well known that low atmospheric pressure has a significant influence on the threshold for lifting dust by aerodynamic drag. Essentially this is based on the lower dynamic pressure available at the low gas density. Usually this is regarded as making it harder to lift dust. However, due to the low atmospheric pressure the dominant processes can change significantly where the flow regime changes at the atmosphere soil interface and within the soil. This effect can offset some of the low-pressure disadvantages and add a lifting component. This "different" regime is accompanied by gas flows, sub-soil overpressures and, therefore, lifting forces.

Important in this context is the ratio between the mean free path of the gas molecules (λ) and the dust or pore diameter (d) within the soil which defines the Knudsen number ($Kn = \lambda / d$). If Kn gets larger or becomes comparable to 1 the usual relation of an ideal gas between pressure P, temperature T and gas density ρ, $P / T \rho$ = (constant), can no longer be applied. The difference can well be illustrated in the case of two chambers, which are connected by a small hole or capillary (Figure 5).

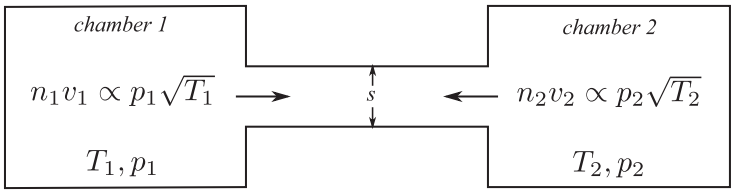

Figure 5. If the connection between two chambers is small compared to the mean free path the pressure in the warm chamber increases because gas flows in the direction from cold to warm (Kelling and Wurm 2009).

If the connection is smaller than the mean free path (*Kn* >> 1) the pressure is no longer the same in both chambers. In this case gas – somewhat counterintuitive – flows from the cold chamber to the warm chamber until the flow balances if $n_1v_1 = n_2v_2$ where n is the particle number density and v the thermal velocity. This corresponds to $P_1/P_2 = (T_2/T_1)^{1/2}$. This type of gas flow along a surface (here the walls of the connecting capillary) is known as thermal creep.

At martian conditions the mean free path is on the order of 10 µm, within the range where low pressure physics (*Kn* ≥ 1) becomes important for dust and sand-sized structures. Therefore, if temperature gradients are present within the martian soil, thermal creep gas flow will move from cold to warm. For comparison, the mean free path for air at 1 bar (terrestrial surface) is only 67 nm. Because typical pore-diameters for sand and soil are much larger than this, thermal creep is not important in natural terrestrial settings.

Where natural thermal creep is concerned, Kelling and Wurm (2014) consider gas pumping by dust clouds in planet formation. More importantly, the martian soil itself could act as a natural pump. Drop tower experiments were used by de Beule et al. (2015) to demonstrate gas flow within soils. Because buoyancy driven, thermal convection does not exist in microgravity, tracer particles immediately visualize the gas flow. Gas inflow was found in cool areas and gas outflow occurred in warm areas (Figure 6).

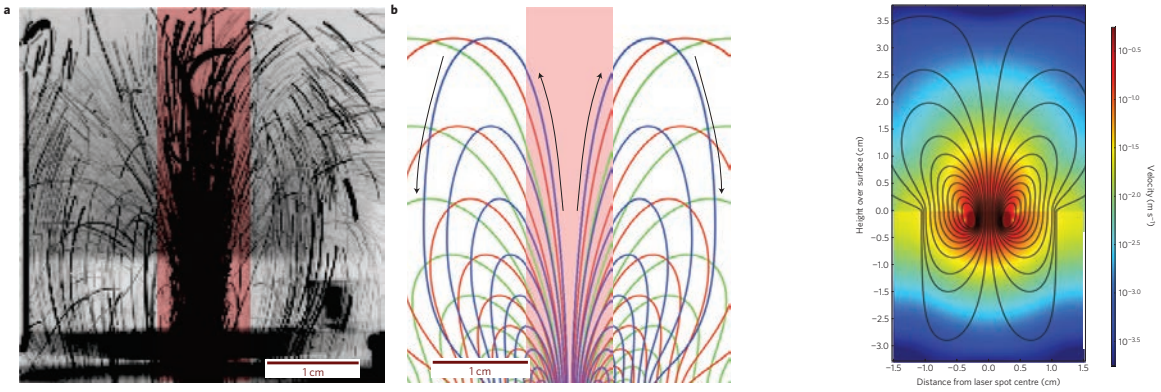

Figure 6. Left: tracer particles in a microgravity experiment. Contours mark the gas flow; Center: simulated gas flow; Right: simulation of temperature and flow above and within dust bed (see de Beule et al. 2015 for details).

Thermal creep is one type of low-pressure process concerning gas motion. The question is if and how this can lead to a dust or sand motion or particle lifting force. The thermal creep gas flow does not directly provide lift within the pumping soil because it requires a temperature gradient to exist. In an insolated soil, a typical temperature gradient might look like Figure 7 (top) with the calculated temperature profile in Figure 8 (taken from de Beule et al., 2015). Kocifaj et al. (2010) provide details on the calculation of this relationship.

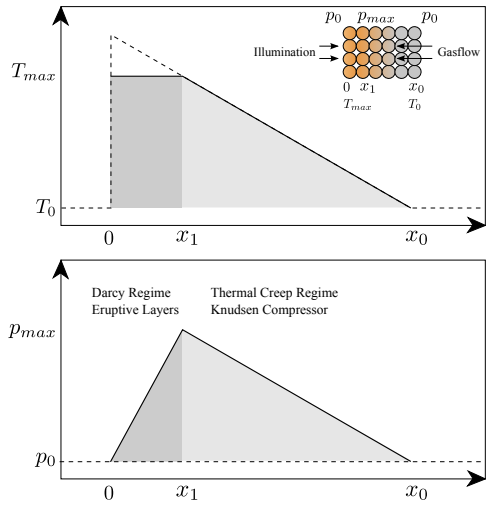

Figure 7. Temperature profile (top) and pressure distribution (bottom) in an insolated dust bed at *Kn* > 1 (schematic, de Beule et al. 2015)

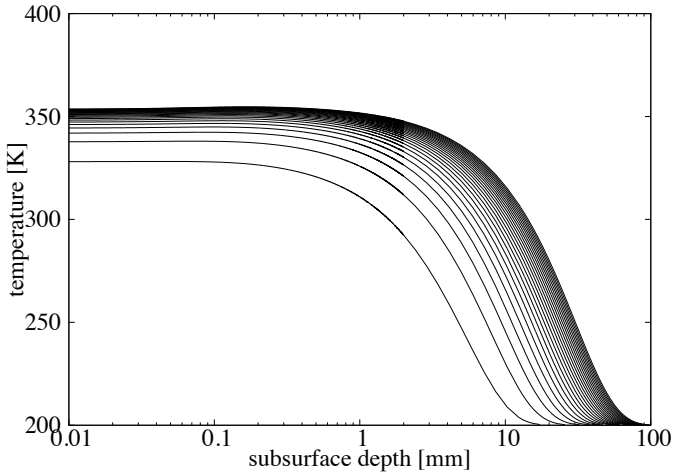

Figure 8. Calculated temperature profile for a dust bed with insolation of 700 W/m^2 up up to 12.5 hours of illumination (de Beule et al. 2015, for details of calculation see Kocifaj et al. 2010).

The top layer does not show a strong temperature variation due to the fact that the surface of the insolated soil can cool by thermal radiation. The thickness of the top layer with constant temperature depends on the duration of illumination. De Beule et al. (2015) find thicknesses of 100 to 200 µm in laboratory settings for seconds of observation but more extended illumination in time (e.g., during a martian day) might lead to mm-thick layers of constant temperature as seen in Figure 8. This is important as the top layer does not pump by thermal creep (no temperature gradient) but the layers below do. Continuity requires that the gas pumped from below pass through the top layer. In the absence of thermal creep, gas flow can only be produced by a pressure-driven gas flow. Therefore, a sub-surface overpressure is established as seen in Figure 7 (bottom). The mass flow rate was described by (Muntz et al. (2002):

$$\dot{M} = p_{avg} \frac{FA}{\sqrt{2\frac{k_B}{m}T_{avg}}} \times \left(\frac{L_r}{L_x} \frac{\Delta T}{T_{avg}} Q_t - \frac{L_r}{L_x} \frac{\Delta p}{p_{avg}} Q_p \right) \tag{4}$$

where *FA* is the surface coverage of pores, T_{avg} is the average temperature, p_{avg} is the average pressure, k_B is the Boltzmann constant, *m* the molecular mass, L_r and L_x are the capillary radius and length, respectively. Equation 4 includes the two terms mentioned: the thermal creep flow

characterized by the non-dimensional gas flow, Q_t, and the pressure difference driven flow characterized by Q_p. It is the pressure difference ΔP, which provides a lift for particles on an illuminated surface on Mars, which is set by the temperature difference along capillaries or pores, ΔT.

This lift can be very strong but as outlined above is generally limited to low, millibar-pressure for soils. Wurm and Krauss (2006) found that particle lift can easily overcome gravity and interparticle forces if essentially any light absorbing dust sample was illuminated with a strong laser beam. Wurm et al. (2008) studied the gravity dependence and applied the results to Mars. An example of the gravity dependence is show in Fig. 9 taken from de Beule et al. 2013. The light flux used in the experiments (12 kW/m^2) is an order of magnitude larger than natural insolation at the martian surface.

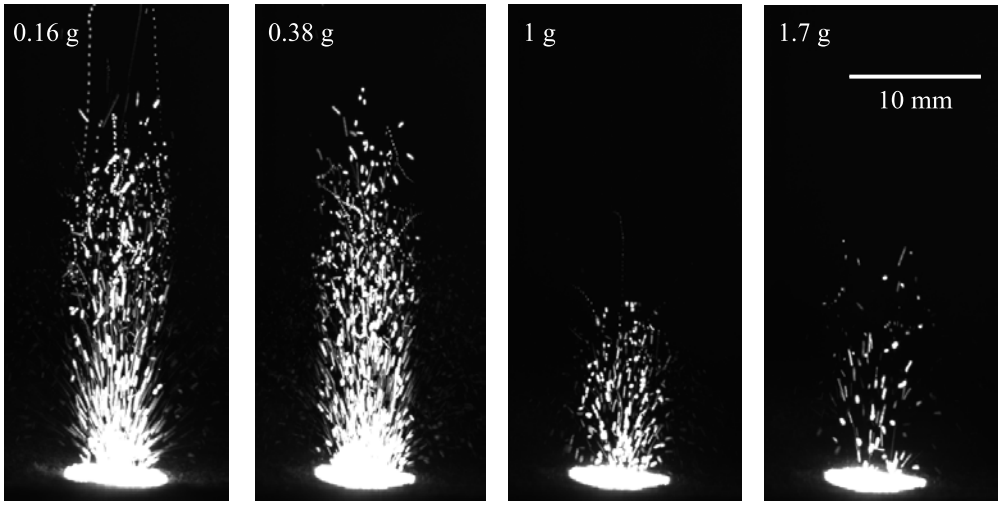

Figure 9. Examples of particle ejections due to illumination at different g-levels (de Beule et al. 2013).

On Earth typically at least a few kW m^{-2} are needed in the laboratory for millibar-pressure to lift dust. In this case no other lifting force is needed, but if the light flux is lower, thermal creep and the pressure gradient are less intense though still present. At low light fluxes below 1 kW m^{-2} the flow is not strong enough on its own to lift particles against gravity (terrestrial or martian) and interparticle forces. De Beule et al. (2015) conducted experiments where a short vibration removed cohesive forces between the particles. As a result, the topmost layers were lifted by the pressure gradient created by thermal pumping. De Beule et al. (2015) call this an insolation-activated layer (Figure 10).

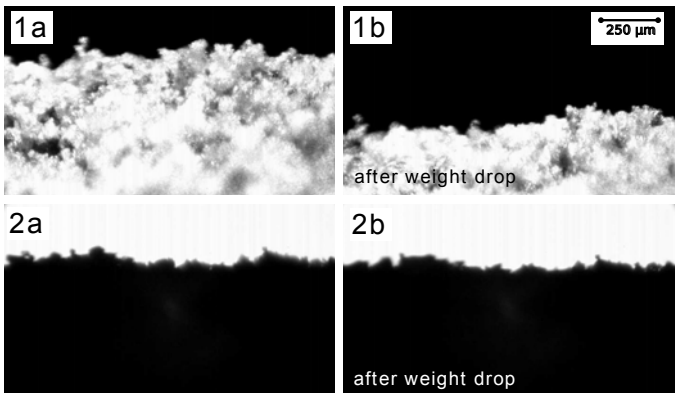

Figure 10. If cohesion is removed, an illuminated dust layer is ejected (1a-1b); the dust layer within a shadowed region does not change as it is not supported by overpressure (2a-2b).

Estimates for martian conditions imply that insolation activation should reduce the threshold velocity for gas drag to lift dust (de Beule et al. 2015). This is consistent with current wind tunnel experiments by Kuepper and Wurm (2015). They studied the threshold friction velocity depending on the insolation

for pressures relevant to Mars. Figure 11 shows the results of their laboratory measurements of threshold friction velocities depending on the insolating flux.

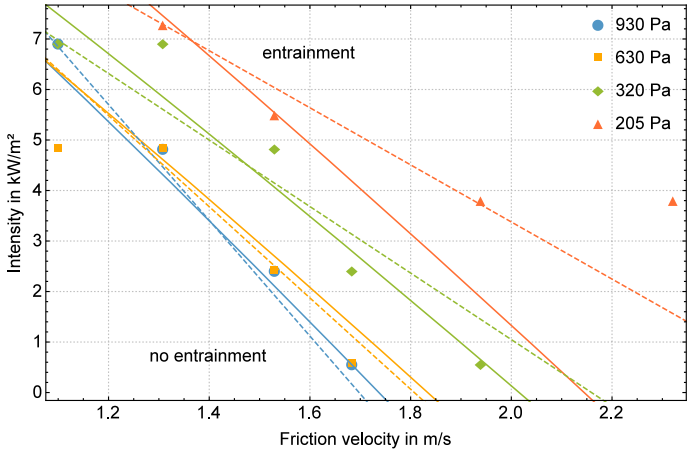

Figure 11. Threshold friction velocities at given light flux and for different pressures (Kuepper and Wurm, 2015).

Scaled to Mars, Kuepper and Wurm (2015) found that illumination can reduce the threshold velocity by between 5% and 18%. Applied to dust devils this means that threshold velocities for translational or rotational motion of the vortex should also be smaller, making them more able to pick up dust.

Once initiated, dust lifting in optically-thick dust devils might be self-sustained. Kelling et al. (2011) and Kocifaj et al. (2010) show that a spontaneous decrease of the light flux can result in stronger particle lift force over a certain time span. Up to 100 times more particles can be released during this period. This is due to the evolving temperature gradient within the soil. That means that as a dust devil traverses and shuts off the sunlight the shadowed dust will be picked up more easily. However, this requires the dust devil to have formed first. It will, though, influence the mass budget of lifted dust but this is in the realm of future studies.

3.2.3 The role of electrodynamics in natural particle lifting

Electrification of particles is another candidate for enhanced lifting in martian dust devils. While being responsible for the mobilization of particles of different sizes, the saltation process favors particle electrification. Indeed, in their ballistic trajectories, particles bounce onto the surface colliding with other grains and exchanging electric charge (Harper, 1967; Renno et al., 2004; Kok and Renno, 2008). The exact mechanism governing this charge exchange is not yet completely understood, but some theoretical models and some experiments suggest this is a size dependent process (Freier, 1960; Schmidt et al., 1998; Inculet et al., 2006; Duff and Lacks, 2008). Consequently, during dusty events, as local turbulence transports the finest particles higher into the atmosphere leaving the more massive grains closer to the surface, the atmosphere experiences a charge separation that produces an enhancement of its electric field. Moreover, some theoretical models and laboratory experiments suggest that the electric forces produced this way can be of the same order of magnitude as gravitational forces, thus being able to influence the trajectories of charged particles (Schmidt et al., 1998; Zheng et al., 2003) and also to reduce the threshold friction velocity u_{*t} necessary to initiate saltation and dust lifting. Electrical forces could thus play a major role in enhancing the particle lifting process (Kok and Renno, 2006).

Recent field experiments (Esposito et al., 2015) monitored the atmospheric electric field during dust events, including saltation, dust storms and devils, observed during an intense field test campaign in the West Sahara. Esposito et al. performed simultaneous measurements of atmospheric parameters (pressure, wind, relative humidity, temperature, solar irradiance, electric field), soil parameters (temperature, moisture), and sand and dust parameters (dust size distribution and abundance, sand saltation rate and flux) during the dust storm seasons in 2013 and 2014 in the desert region of

Merzouga in Morocco. They observed a very strong correlation between saltation rate and dust emission, and between these two parameters and the intensity of the atmospheric electric field. This demonstrated both the role of saltation in the dust emission and the particle electrification processes acting during these phenomena (Figure 12).

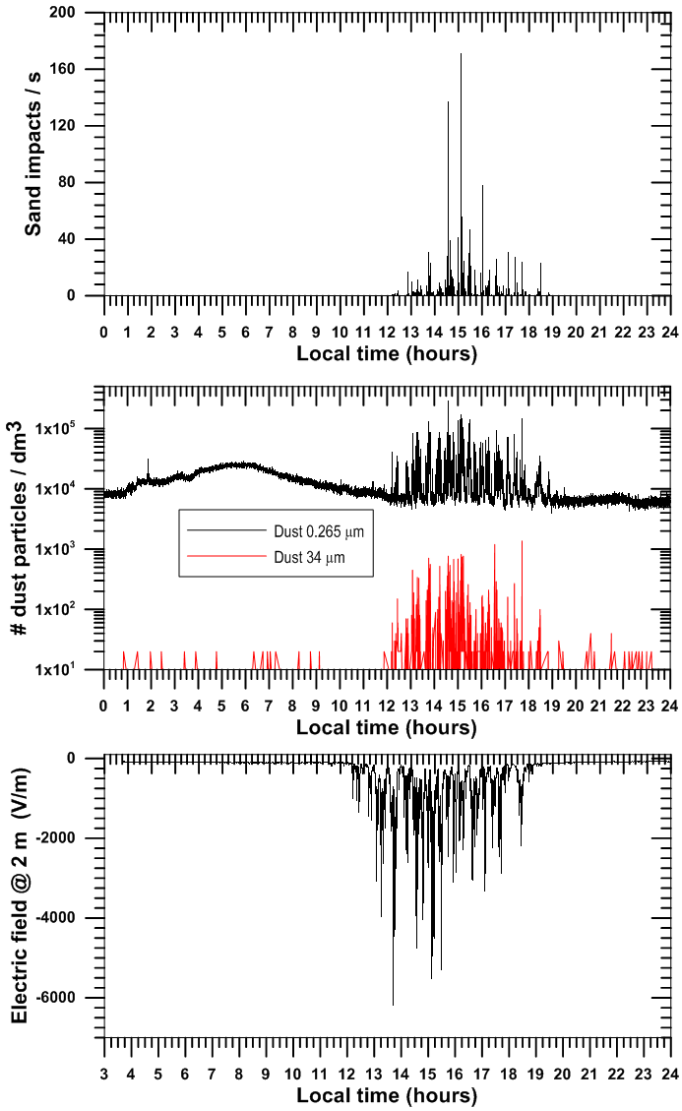

Figure 12: Typical dust storm observed in the Moroccan desert (Esposito et al., 2015): sand saltation rate, atmospheric dust concentration and electric field at 2 m from the ground versus time.

Esposito et al., (2015) observed E-fields up to 15 kV/m during the strongest dust events as measured by a field mill mounted two meters above the ground, similar to what has been reported by other observers (Rudge, 1913; Demon et al., 1953; Stow, 1969; Kamra, 1972; Williams et al., 2009). E-fields were generally directed in the downward direction, the same as the fair-weather field. A linear trend was observed between dust abundance and the E-field shown in Figure 13.

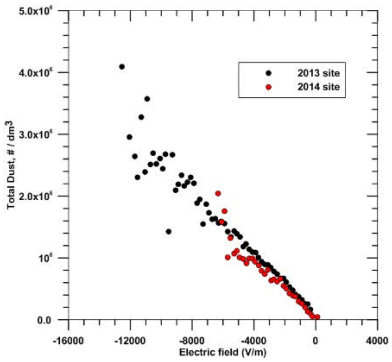

Figure 13: Atmospheric dust concentration as a function of the electric field. Data acquired in two different sites in the desert region of Merzouga (Morocco) respectively in 2013 and 2014 (Esposito et al., 2015) in dry conditions (relative humidity below 10%).

The observed trend was almost the same in both years 2013 and 2014 campaigns even if the two measurement sites were different in terms of soil moisture content and composition. This testifies the effect of the electrification of fresh lifted dust on the electric properties of the atmosphere. A similar trend was observed in dust devils (see Murphy et al., *this issue*).

Although it is thought that electrification of dust is typical during mobilization and that it can be instrumental in the formation of dust aggregates (see Harrison et al., *this issue*) it has yet to be implemented into a predictive model.

3.2.4 ∆P-Effect, Revisited

As has been shown, the added lift component from vortex action, originally dubbed the "∆*P-effect*", is most likely a complex interaction of several factors resultant from the passage of the dust devil over the surface. As such, it is perhaps better to designate this combined lifting effect the "enhanced vortex entrainment effect" (EVE-effect). Any or all of the contributing factors could be active in any given dust devil, contributing to rates of change for each process. Pressure-excursion effects such as those proposed by Greeley et al. (2003) could be explained in part by Balme and Hagermann (2006) as mechanical pressure equalization, where the 'trapping' of pockets of gas beneath a low pressure zone within a dust devil lifts particles into the flow. Furthermore, vortex-induced particle lifting could occur by some combination of those mechanical processes with varying contributions from thermo-luminescent (e.g., Küpper and Wurm (2015) or electrodynamic processes (e.g., Esposito et al., 2015). The EVE-effect is thus not only a function of the vortex properties, but also in part, the surface materials and the ambient atmospheric conditions. Availability of sediment, pore space within the sediment, surface roughness, and sediment intrinsic properties (e.g., particle size and density distributions, moisture content, electrical properties, etc.) all influence how the surface responds to the passage of a convective vortex and whether or not that vortex becomes a dust devil by entraining sand and dust. Background ambient atmospheric conditions add to this effect by externally controlling the formation of the convective vortex. All of these factors are important to consider for designing new multi-tiered, co-registered observations in the field and laboratory to separate individual factors better for consideration within analytical models.

3.3 Analytical Modeling

As outlined in Section 2, aerodynamic entrainment, saltation bombardment, and aggregate disintegration processes can contribute to dust emission in dust devils. On Earth, saltation bombardment and aggregate disintegration are the most effective dust emission mechanisms (Gillette et al., 1974; Shao et al., 1993) and have thus been the main focus of research. Both require saltation as an intermediate process.

On Mars, the mechanics of dust lifting are quite different from those on Earth. In particular, because of Mars' low atmospheric density, formidable wind speeds of the order of $u_{*t} \approx 2$ m/s are needed to initiate saltation. However, numerical modeling indicates that, once initiated, saltation (and thus dust emission) can be sustained by wind speeds that are an order of magnitude less intense (Claudin and Andreotti, 2006; Almeida et al., 2008; Kok, 2010a, b). The Earth-like size of ripples encountered by

Mars rovers (e.g., Sullivan et al., 2005) are consistent with this resulting hysteresis in martian sand transport (Yizhaq et al., 2014). Nonetheless, the extent of the role that saltation plays in dust lifting in martian dust devils and dust storms remains unclear. Indeed, observations by Sullivan et al. (2008) indicate that dust emission regularly occurs without saltation, namely by the aerodynamic entrainment of low-density sand-sized aggregates of dust that has settled from the sky (also see Merrison et al., 2007). Here the EVE-effect is not taken into account – only the surface shear stresses caused by the swirling winds within the dust devil are considered.

Below, we discuss parameterizations of dust emission through either saltation bombardment and aggregate fragmentation (3.3.1) or direct aerodynamic entrainment (3.3.2). These parameterizations have been developed for Earth, where observations are available to test them. The parameterization of dust lifting by dust devils and larger-scale winds in martian atmospheric circulation models is generally more primitive, in part because of the lack of observations, and in part because of the aforementioned remaining fundamental questions regarding the mechanics of martian dust lifting (Mulholland et al., 2015).

3.3.1 Parameterizations of dust emission due to saltation bombardment and aggregate disintegration

Due to their hopping motion, the effective movement of saltating grains is in the horizontal wind direction and is expressed as a horizontal saltation flux, Q. For smaller dust devils, saltating particles might be expelled from the bottom of the vortex quite rapidly, but in larger ones, wind speeds are intense enough to make sand grains follow broad curving paths within the dust devil. In parameterization schemes, saltation is typically described as a uniform equilibrium process based on the momentum balance in the saltation layer, a layer close to the surface covering the height of most saltation trajectories (Owen, 1964), though the accuracy of this simplifying assumption has been questioned by recent studies (e.g., Barchyn et al., 2014). Most studies, starting with Bagnold (1941), have suggested that Q is proportional to the cube of the friction velocity (u_*) (Kawamura, 1951; Owen, 1964; Lettau and Lettau, 1978; Raupach and Lu, 2004). However, more recent work has suggested a dependence on the square of the friction velocity (Ungar and Haff, 1987; Ho et al., 2011; Duran et al., 2011; Kok et al., 2012). Unfortunately, the scatter in wind and field tunnel measurements is generally such that no firm conclusion can be reached on the exact dependence of the horizontal sand flux on soil state and wind speed (e.g., Iversen and Rasmussen, 1999; Kok et al., 2012).

The vertical dust emission flux, F, generated by saltation bombardment (also known as abrasion) or aggregate disintegration (auto-abrasion) is dependent on the horizontal saltation flux, Q, as the energy transferred to the surface by saltating grains at impact determines the energy available for dust lifting (e.g., Shao et al., 1993; Marticorena and Bergametti, 1995). Thus, F is often expressed as

$$F(d_i, d_s) = \alpha(d_i, d_s)Q(d_s) \quad (5)$$

where d_i denotes the diameter of dust particles, and d_s that of saltating grains (Shao, 2004). The determination of α is the major challenge addressed in saltation-based dust emission parameterizations.

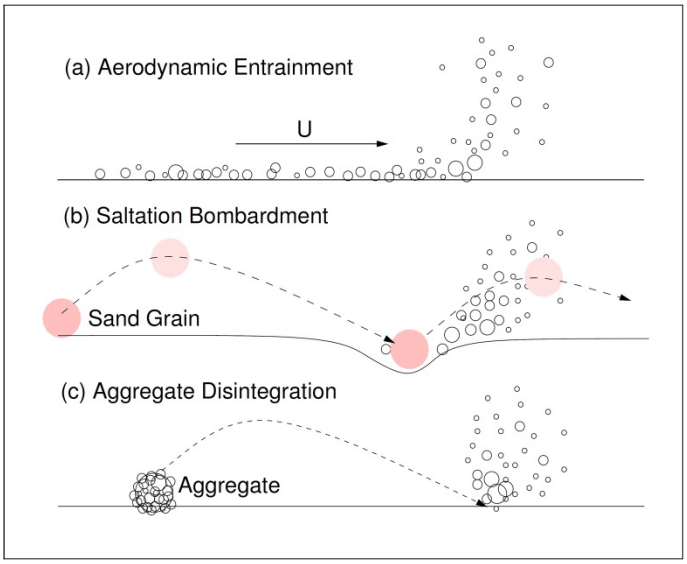

Figure 14. Illustration of (a) dust emission by aerodynamic lift, (b) by saltation bombardment, and (c) through aggregate disintegration. Modified from Shao (2008).

Marticorena and Bergametti (1995) proposed a semi-empirical dust emission parameterization. The authors suggest that the magnitude of *F* depends on dust particle abundance at the surface and relate α to soil clay content. Other studies propose physically-explicit parameterizations. For example, Shao et al. (1993, 1996) and Alfaro and Gomes (2001) relate α to the binding energy, ψ, of the particles at the surface, $\alpha \propto \beta / \psi$, where β is a parameter.

Shao (2001, 2004) explicitly consider both saltation bombardment and aggregate disintegration. The bombardment process is described in terms of the volume removal at the soil surface through impacting grains based on the work of Lu and Shao (1999) (Figure 15a). Whether dust is emitted through abrasion or aggregate disintegration is determined by the mass fraction of free/aggregated dust available. The size of the volume that can be removed depends on the resistance the saltating grain experiences at impact. As a consequence, α is based on soil texture and soil plastic pressure in the scheme of Shao (2001, 2004).

More recently, Kok (2011b) proposed that most dust aerosol emission results from the fragmentation of aggregates of dust particles, which can occur either from impacts of saltators onto these aggregates, or from the saltation of these aggregates themselves (Figure 15b). This analogy with the well-studied phenomenon of brittle material fragmentation (Astrom, 2006) allowed the derivation of a simple analytical expression for the size distribution of emitted dust aerosols that eliminates some of the complexities of previous schemes, while being in good agreement with available measurements (also see Mahowald et al., 2014). Kok et al. (2014b) then built on this hypothesis that most dust emission results from aggregate fragmentation to propose a new theoretical model for how the dust flux emitted by an eroding soil depends on wind and soil properties. In this model, the efficiency with which the horizontal saltation flux produces a vertical dust flux depends primarily on soil clay content, which determines the dust mass available for disaggregation, and on the soil binding energy, which determines the resistance of the soil to fragmentation. This new dust emission model improves the representation of the global dust cycle in the Community Earth System Model (Kok et al., 2014a).

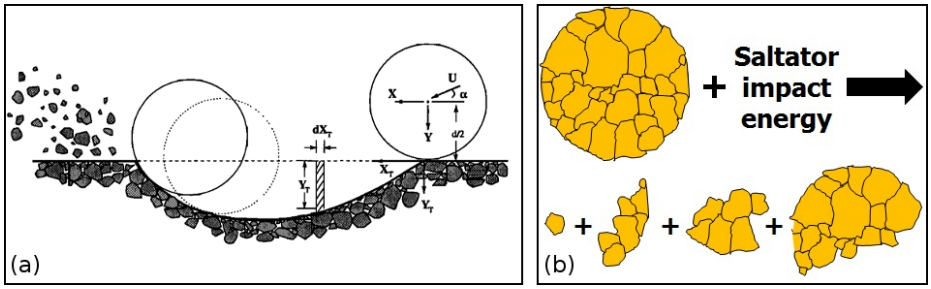

Figure 15. (a) Illustration of dust emission via soil volume removal by impacting saltating grains during saltation bombardment as described by Shao (2001, 2004) (from Shao, 2001); (b) Illustration of dust emission through soil or saltation aggregate disintegration in analogy with brittle fragmentation as described by Kok (2011b) and Kok et al. (2014b).

All schemes have been proven valuable for the modeling of regional and/or global-scale dust patterns, such as dust storms (e.g. Cavazos et al., 2009; Shao et al., 2010; Kok et al., 2014b). Their application to small-scale dust events, such as dust devils, can however be problematic due to the intermittent nature of atmospheric turbulence being pivotal on small and micro scales (e.g., Barchyn et al., 2014).

3.3.2 Parameterizations of dust emission due to aerodynamic entrainment

In the absence of saltation, i.e. in the situation of $u_* < u_{*t}$, the above-mentioned dust emission schemes do not predict any dust emission. Observations show, however, that saltation can occur intermittently even though u_* is on average smaller than u_{*t} and that dust can also be aerodynamically entrained (Stout and Zobeck, 1997; Loosmore and Hunt, 2000; Macpherson et al., 2008; Cameiro et al., 2014).

Intermittently large momentum fluxes are due to atmospheric turbulence, which is most coherent in the case of unstable atmospheric stratification or in the presence of roughness elements (Stull, 1988; Raupach et al., 1996). Klose and Shao (2012) and Klose et al. (2014) developed a parameterization for the direct aerodynamic entrainment of dust with a focus on convective turbulent conditions. Dust emission is described as a stochastic process by representing both inter-particle cohesive forces and aerodynamic lifting forces, i.e. momentum fluxes due to atmospheric turbulence, as probability distributions. Dust emission fluxes produced by the scheme are mostly two to three orders of magnitude smaller than fluxes typically obtained for saltation-generated dust emission. However, under favorable conditions such as in dust devils, fluxes can be of similar magnitude and have been found to be close to those observed in the field (Klose and Shao, 2015). Intermittent saltation is not yet included in the scheme and would further increase modeled turbulent dust emission.

Wang (2016) compared the friction and horizontal pressure forces acting in a dust devil and found that friction forces exceeded horizontal pressure forces. The author derived a theoretical expression for the direct aerodynamic entrainment of dust in dust devils based on the Navier-Stokes equations for a rotating flow and obtain larger emissions for direct aerodynamic entrainment than for dust emission generated by saltation bombardment. However, inter-particle cohesion has been neglected in the approach of Wang (2016), so his estimate of aerodynamic dust emission is likely an overestimation.

4. Conclusions & Future Work

Particle lifting and entrainment within dust devils are complicated processes that result from the internal balancing of multiple subsidiary processes, all of which may or may not be active in any given dust devil. The complex nature of these interactions mean they are difficult to separate and study in the context of dust devils on Earth and Mars. Nevertheless, interactions between the various dust devil communities has led to advances that incorporate field observations on both planets, laboratory experiments (at terrestrial ambient and Mars analog conditions), and analytical modeling, clarifying many of the component processes for sediment transport within dust devils. The so-called ΔP-effect, describing the 'suction' of a low-pressure core within a dust devil, is perhaps better described as the EVE-effect (enhanced vortex entrainment), as it is actually a combination of many processes resulting from the conditions associated with the passage of dust devil over the surface. This is intimately tied to the rate of change in the processes interacting with the surface, which leads to varying amounts of sediment lifting depending on the strength and translation speed of the dust devil. The amount of dust in the dust devil could also have an effect through electrification-processes and the strength and speed of the dust devil is in turn tied to both the ambient conditions necessary for producing the vorticity and pressure structure within the dust devil and the instantaneous interactions between the lifting potential of the flow and the heterogeneous characteristics of sediment on the surface. The dust load, and even the orientation of the dust devil with respect to the sun, might have an additional effect, as the thermo-luminescent effect described above might be enhanced by sudden shadowing of the surface as the dust devil passes. The dominant form of lifting within a single dust devil could be dominated by pore-space pressure equalization or thermo-luminescent enhanced lifting or mechanical saltation bombardment, but it is likely the feedback of each of these within the dust devil which helps

fuel many of the other processes ongoing within the vortex, and ultimately leading to dust lifting and the production of a 'classical' dust devil column.

Dust devils have been demonstrated to be intrinsically different lifting phenomena (see Chapter 1) compared to boundary layer winds. Through experiments and observations dust devils have been identified as effective lifters of dust given the proper conditions on Earth and Mars, and have been shown to be capable of removing dust on spacecraft solar panels. One of the more difficult remaining questions for dust devil studies involves discerning the individual roles of each of the component processes acting at any given time in dust devils. The difficulty arises in the ability to simultaneously collect bulk data on both the internal properties via in situ sensor suites (e.g., how pressure, wind velocities and particle counts are changing with time) and external measurements of how the dust composition, size distributions, and flux are changing over the lifetime of a dust devil. Future observations will need to make better use of combined networks of sensors and camera systems to better characterize dust devil populations by attempting to get both types of data simultaneously. Laboratory studies can aid in development of instrumentation for these types of networks. Laboratory studies can also continue to refine our knowledge about the individual component processes by further isolation of specific variables including mechanical versus thermal versus electrodynamical dust lifting mechanisms. Analytical modeling can continue to evolve with better computational ability and improved inputs from both observations and laboratory experiments. Analytical modeling serves the important role of connecting what we know about the specific processes to the larger regional and global systems and helps to define how dust devils result from and are tied to the bigger picture.

Acknowledgments
This work was supported by grant National Science Foundation grant AGS-1358621 to J. K.

References
Alfaro, S. C., and L. Gomes (2001), Modeling mineral aerosol production by wind erosion: Emission intensities and aerosol size distributions in source areas, J. Geophys. Res., 106 (D16), 18,075-18,084.

Allen, C.J.T., R. Washington, and A. Saci (2015), Dust detection from ground-based observations in the summer global dust maximum: Results from Fennec 2011 and 2012 and implications for modeling and field observations, *J. Geophys. Res.*, 120, 897-916, doi:10.1002/2014JD022655.

Almeida M.P., E.J.R. Parteli, J.S. Andrade and H.J. Herrmann (2008), Giant saltation on Mars, *Proc. Natl Acad. Sci. USA*, 105 6222–6.

Arya, S. P. S. (1975), A drag partition theory for determining the large-scale roughness parameter and wind stress on the Arctic pack ice, J. Geophys. Res., 80 (24), 3447-3454, doi:10.1029/ JC080i024p03447.

Astrom, J.A., (2006), Statistical models of brittle fragmentation. Advances in Physics 55, 247-278.

Bagnold, R. A. (1941), The Physics of Blown Sand and Desert Dunes, 265 pp., Methuen, London.
Balme, M., S. Metzger, M. Towner, T. Ringrose, R. Greeley, and J. Iversen (2003), Friction wind speeds in dust devils: A field study, Geophysical Research Letters, 30 (16), doi:10.1029/ 2003GL017493, 1830.

Balme, M.R., Metzger, S.M., Towner, M.C., Ringrose, T.J., Greeley, R., Iversen, J.D., (2003b). Friction wind speeds in dust devils: A field study. Geophys. Res. Lett. 30. doi:10.1029/2003GL017493.

Balme, M. and A. Hagermann (2006), Particle lifting at the soil-air interface by atmospheric pressure excursions in dust devils, *Geophys. Res. Lett.*, 33, L19S01, doi:10.1029/2006GL026819.

Balme, M.R., A. Pathare, S.M. Metzger, M.C. Towner, S.R. Lewis, A. Spiga, L.K. Fenton, N.O. Renno, H.M. Elliott, F.A. Saca, T.I. Michaels, P. Russell, and J. Verdasca (2012), Field measurements of horizontal forward motion velocities of terrestrial dust devils: Towards a proxy for ambient winds on Mars and Earth, *Icarus*, 221, 2, 632-645, doi:10.1016/j.icarus.2012.08.021.

Barchyn, T.E., R.L. Martin, J.F. Kok, and C.H. Hugenholtz, (2014), Fundamental mismatches between measurements and models in aeolian sediment transport prediction: The role of small-scale variability. Aeolian Research 15, 245-251.

Cantor, B.A., K.M. Kanak, and K.S. Edgett (2006), Mars Orbiter Camera observations of Martian dust devils and their tracks (September 1997 to January 2006) and evaluation of theoretical vortex models, *J. Geophys. Res.*, 111, E12, doi:10.1029/2006JE002700.

Carneiro, M.V., K. R. Rasmussen, H.J., H.J. Herrmann (2015), Bursts in discontinuous aeolian saltation, *Scientific Reports*, 5.

Castellanos, A. (2005), The relationship between attractive interparticle forces and bulk behaviour in dry and uncharged fine powders, *Adv. in Phys.*, 54, 4, doi: 10.1080/17461390500402657.

Cavazos, C., M. C. Todd, and K. Schepanski (2009), Numerical model simulation of the Saharan dust event of 6-11 March 2006 using the Regional Climate Model version 3 (RegCM3), J. Geophys. Res., 114 (D12109), doi:10.1029/2008JD011078.

Chepil, W.S., (1945), Dynamics of wind erosion .2. Initiation of soil movement. Soil Science 60, 397-411.

Chkhetiani, O. G., E. B. Gledzer, M. S. Artamonova, and M. A. Iordanskii (2012), Dust resuspension under weak wind conditions: direct observations and model, Atmos. Chem. Phys., 12, 5147-5162, doi:10.5194/acp-12-5147-2012.

Claudin P. and B. Andreotti (2006), A scaling law for aeolian dunes on Mars, Venus, Earth, and for subaqueous ripples, *Earth Planet. Sci. Lett.*, 252, 30–44.

Cornelis, W. M., D. Gabriels, and R. Hartmann (2004a), A conceptual model to predict the deflation threshold shear velocity as a affected by near-surface soil water: I. Theory, Soil Sci. Soc. Am. J., 68, 1154-1161.

Cornelis, W. M., D. Gabriels, and R. Hartmann (2004b), A parameterisation for the threshold shear velocity to initiate deflation of dry and wet sediment, Geomorphology, 59, 43-51, doi: 10.1016/j.geomorph.2003.09.004.

De Beule, C., T. Kelling, G. Wurm, J. Teiser, and T. Jankowski (2013), From Planetesimals to Dust: Low Gravity Experiments on Recycling Solids at the Inner Edge of Protoplanetary Disks, *Astrophysical Journal*, 763:11 1-8.

De Beule, C., G. Wurm, T. Kelling, M. Küpper, T. Jankowski, and J. Teiser (2014), The Martian Soil as a Planetary Gas Pump, *Nature Physics*, 10:17-20.

De Beule, C., G. Wurm, T. Kelling, M. Köster, and M. Kocifaj (2015), An Insolation Activated Dust Layer on Mars, *Icarus*, 260, 23-28.

De Vet, S. J., Merrison, J. P., Mittelmeijer-Hazeleger, M. C., van 460 Loon, E. E., and Cammeraat, L. H. (2014), Effects of rolling on wind-induced detachment thresholds of volcanic glass on Mars: Planetary and Space Science, v. 103, no. 0, p. 205-218

Demon, L., P. Defelice, H. Gondet, Y. Kast, L. Pontier (1953), *Journal des Recherches du C.N.R.S.,* 24, 126.

Duff, N., and D.J. Lacks (2008), Particle dynamics simulations of triboelectric charging in granular insulator systems. *J. Electrost*. 66, 51. doi:10.1016/j.elstat.2007.08.005

Dupont, S., G. Bergametti, B. Marticorena, and S. Simoëns (2013), Modeling saltation intermittency, J. Geophys. Res. Atmos., 118, 7109{7128, doi:10.1002/jgrd.50528.

Duran, O., Claudin, P., Andreotti, B. (2011), On aeolian transport: Grain-scale interactions, dynamical mechanisms and scaling laws. Aeolian Research 3, 243-270.

Ellehoj, M.D., H.P. Gunnlaugsson, P.A. Taylor, H. Kahanpää, K.M. Bean, B.A. Cantor, B.T. Gheynani, L. Drube, D. Fisher, A.-M. Harri, C. Holstein-Rathlou, M.T. Lemmon, M.B. Madsen, M.C. Malin, J. Polkko, P.H. Smith, L.K. Tamppari, W. Weng, and J. Whiteway (2010), Convective vortices and dust devils at the Phoenix Mars mission landing site, *J. Geophys. Res.*, 115, E00E16, doi:10.1029/2009JE003413.

Esposito et al. (2015), *In preparation.*

Fécan, F., B. Marticorena, and G. Bergametti (1999), Parameterization of the increase of the aeolian erosion threshold wind friction velocity due to soil moisture for arid and semi-arid areas, Ann. Geophysicae, 17, 149-157.

Fratini, G., M. Santini, P. Ciccioli and R.Valentini (2009), Evaluation of a wind erosion model in a desert area of northern Asia by eddy covariance, Earth Surf. Proc. Land. , 34, 13, 1743-1757, DOI: 10.1002/esp.1857.

Freier, G.D. (1960), The electric field of a large dust devil. *J. Geophys. Res*. 65, 3504. doi:10.1029/JZ065i010p03504

Gillette, D. A. (1974), On the production of soil wind erosion aerosols having the potential for long range transport, Journal de Recherches Atmospheriques, 8, 735-744.

Gillette, D., I. H. Blifford and C. R. Fenster (1972,) Measurements of aerosol size distributions and fluxes of aerosols on land subject to wind erosion, *J. Appl. Meteorol*., 11, 977–987.

Gillette, D.A., I.H. Blifford, and D.W. Fryrear (1974), Influence of wind velocity on size distributions of aerosols generated by wind erosion of soils. Journal of Geophysical Research 79, 4068-4075.

Gillette, D. A., and R. Passi (1988), Modeling dust emission caused by wind erosion, J. Geophys. Res., 93 (D11), 14,233-14,242, doi:10.1029/JD093iD11p14233.

Ginoux, P., Chin, M., Tegen, I., Prospero, J.M., Holben, B., Dubovik, O., Lin, S.J. (2001), Sources and distributions of dust aerosols simulated with the GOCART model. J. Geophys. Res.-Atmos. 106, 20255-20273.

Greeley, R. and J.D. Iversen (1985), *Wind as a Geologic Process on Earth, Mars, Venus, and Titan*, Cambridge Univ. Press, New York.

Greeley, R., M.R. Balme, J.D. Iversen, S. Metzger, R. Mickelson, J. Phoreman, and B. White (2003), Martian dust devils: Laboratory simulations of particle threshold, *J. Geophys. Res.*, 108, E5, 5041, doi:10.1029/2002JE001987.

Hamaker, H.C. (1937), The London - Van Der Waals attraction between spherical particles. Physica 4, 1058-1072.

Han, Y. L (2006), Investigation of Micro/Meso-scale Knudsen Compressors at Low Pressures (ProQuest Information and Learning Company).

Harper, W. R. (1967), Contact and Frictional Dissipation (Clarendon Press, Oxford).

Hess, G. D., and K. T. Spillane (1990), Characteristics of dust devils in Australia, J. Appl. Meteor., 29, 498-507, doi:10.1175/1520-0450(1990)029h0498:CODDIAi2.0.CO;2.

Ho, T.D., A. Valance, P. Dupont, and A.O. El Moctar (2011), Scaling Laws in Aeolian Sand Transport. Physical Review Letters 106.

Holstein-Rathlou, C., Gunnlaugsson, H.P., Merrison, J.P., Bean, K.M., Cantor, B.A., Davis, J.A., Davy, R., Drake, N.B., Ellehoj, M.D., Goetz, W., Hviid, S.F., Lange, C.F., Larsen, S.E., Lemmon, M.T., Madsen, M.B., Malin, M., Moores, J.E., Nørnberg, P., Smith, P., Tamppari, L.K., and Taylor, P.A. (2010), Winds at the Phoenix landing site, *J. Geophys. Res.*, 115, E00E18

Huneeus, N., M. Schulz, Y. Balkanski, J. Griesfeller, J. Prospero, S. Kinne, S. Bauer, O. Boucher, M. Chin, F. Dentener, T. Diehl, R. Easter, D. Fillmore, S. Ghan, P. Ginoux, A. Grini, L. Horowitz, D. Koch, M.C. Krol, W. Landing, X. Liu, N. Mahowald, R. Miller, J.J. Morcrette, G. Myhre, J. Penner, J. Perlwitz, P. Stier, T. Takemura, and C.S. Zender (2011), Global dust model intercomparison in AeroCom phase I. *Atmospheric Chemistry and Physics* 11, 7781-7816.

Hurrell, J.W., M.M. Holland, P.R. Gent, S. Ghan, J.E. Kay, P.J. Kushner, J.F. Lamarque, W.G. Large, D. Lawrence, K. Lindsay, W.H. Lipscomb, M.C. Long, N. Mahowald, D.R. Marsh, R.B. Neale, P. Rasch, S. Vavrus, M. Vertenstein, D. Bader, W.D. Collins, J.J. Hack, J. Kiehl, and S. Marshall, (2013), The Community Earth System Model A Framework for Collaborative Research. *Bulletin of the American Meteorological Society* 94, 1339-1360.

Ibrahim, A.H., Dunn, P.F. and Qazi, M.F. (2008), Experiments and validation of a model for microparticle detachment from a surface by turbulent air flow, Aerosol Science, 39, 645-656.

Inculet, I.I., G.S. Peter Castle, G. Aartsen (2006), Generation of bipolar electric fields during industrial handling of powders. *Chem. Eng. Sci.* 61, 2249–2253. doi:10.1016/j.ces.2005.05.005

Ishizuka, M., M. Mikami, J. Leys, Y. Yamada, S. Heidenreich, Y. Shao, and G. H. McTainsh (2008), Effects of soil moisture and dried raindroplet crust on saltation and dust emission, J. Geophys. Res., 113, D24212, doi:10.1029/2008JD009955.

Ishizuka M., M. Mikami, J. F. Leys, Y. Shao, Y. Yamada, S. Heidenreich (2014), Power law relation between size-resolved vertical dust flux and friction velocity measured in a fallow wheat field, Aeol. Res., 12, 87–99.

Iversen, J., J. Pollack, R. Greeley, and B. White (1976), Saltation threshold on Mars: The effect of interparticle force, surface roughness, and low atmospheric density, *Icarus*, 29 (3), 381-393, doi:http://dx.doi.org/10.1016/0019-1035(76)90140-8.

Iversen, J.D. and K.R. Rasmussen (1999). The effect of wind speed and bed slope on sand transport. *Sedimentology* 46, 723-731.

Iversen, J. D., and B. R. White (1982), Saltation threshold on Earth, Mars and Venus, *Sedimentology*, 29, 111-119.

Jemmett-Smith, B.C., J.H. Marsham, P. Knippertz, and C.A. Gilkeson (2015), Quantifying global dust devil occurrence from meteorological analyses, *Geophy. Res. Lett.*, 42, 1275-1282, doi:10.1002/2015GL063078.

Johnson, K.L., K. Kendall, and A.D. Roberts (1971), Surface energy and contact of elastic solids. *Proceedings of the Royal Society of London Series a-Mathematical and Physical Sciences* 324, 301-&.

Johnson, J.R., W.M. Grundy, and M.T. Lemmon (2003), Dust deposition at the Mars Pathfinder landing site: observations and modeling of visible/near-infrared spectra, *Icarus* 163, 330-346.

Kahn, R.A., T.Z. Martin, R.W. Zurek, and S.W. Lee (1992), The Martian dust cycle, in *Mars*, ed. H. Kieffer et al., Ch. 29, 1017-1053, Univ. of Ariz. Press, Tucson.

Kahre, M.A., J.R. Murphy, R.M. Haberle (2006), Modeling the Martian dust cycle and surface dust reservoirs with the NASA Ames general circulation model, *J. Geophys. Res.*, 111, E06008, doi:10.1029/2005JE002588.

Kaimal, J.C., and J.J. Finnigan (1994), Atmospheric boundary layer flows: Their structure and measurement Oxford Univ. Press, New York.

Kamra, A. K. (1972), Measurements of the Electrical Properties of Dust Storms. *J. Geophys. Res.*, Vol. 77, No. 30, 5856.

Kelling, T., and G. Wurm (2009), Self-sustained Levitation of Dust Aggregate Ensembles by Temperature Gradient Induced Overpressures, *Physical Review Letters*, 103:215502 1-4.

Kelling, T., and G. Wurm (2011), A Mechanism to Produce the Small Dust Observed in Protoplanetary Disks, *Astrophysical Journal*, 733:120-124.

Kelling, T., G. Wurm, M. Kocifaj, J. Klačka, and D. Reiss, Dust Ejection from Planetary Bodies by Temperature Gradients: Laboratory Experiments, *Icarus*, 212:935-940, 2011.

Kelling, T., and G. Wurm, Accretion through the Inner Edge of a Protoplanetary Disk by a Giant Solid State Pump, *Astrophysical Journal Letters*, 774:L1 1-2, 2013.

Klose, M., and Y. Shao (2012), Stochastic parameterization of dust emission and application to convective atmospheric conditions, *Atmos. Chem. Phys.*, 12 (12), 7309-7320, doi:10.5194/acp-12-7309-2012.

Klose, M., and Y. Shao (2013), Large-eddy simulation of turbulent dust emission, *Aeolian Research*, 8, 49-58, doi:10.1016/j.aeolia.2012.10.010.

Klose, M., Y. Shao, X. L. Li, H. S. Zhang, M. Ishizuka, M. Mikami, and J. F. Leys (2014), Further development of a parameterization for convective turbulent dust emission and evaluation based on field observations, *J. Geophys. Res. Atmos*., 119, 10,441-10,457, doi:10.1002/2014JD021688.

Klose, M. R. (2014), Convective Turbulent Dust Emission: Process, parameterization, and relevance in the Earth system, Dissertation, University of Cologne, urn:nbn:de:hbz:38-58264.

Kocifaj, M., J. Klačka, G. Wurm, T. Kelling, and I. Kohút (2010), Dust Ejection from (Pre-) Planetary Bodies by Temperature Gradients: Radiative and Heat Transfer, *Monthly Notice of the Royal Astronomical Society*, 404:1512-1518.

Kocifaj, M., J. Klačka, T. Kelling, and G. Wurm (2011), Radiative Cooling within Illuminated Layers of Dust on (Pre)-Planetary Surfaces and its Effect on Dust Ejection, *Icarus*, 211:832-838.

Knudsen, M. (1909), *Ann. Phys.* (Leipzig) 336, 205.

Kok, J.F. (2010a), An improved parameterization of wind-blown sand flux on Mars that includes the effect of hysteresis *Geophys. Res. Lett.,* 37, L12202.

Kok, J.F. (2010b), Difference in the wind speeds required for initiation versus continuation of sand transport on Mars: implications for dunes and dust storms, *Phys. Rev. Lett.*, 104, 074502.

Kok, J.F. (2011a), Does the size distribution of mineral dust aerosols depend on the wind speed at emission?, *Atmospheric Chemistry and Physics*, 11, 10149-10156.

Kok, J. F. (2011b), A scaling theory for the size distribution of emitted dust aerosols suggests climate models underestimate the size of the global dust cycle, *Proceedings of the National Academy of Sciences (PNAS)*, 108(3), 1016-21.

Kok, J.F., Renno, N.O. (2006), Enhancement of the emission of mineral dust aerosols by electric forces. *Geophys. Res. Letters*, 33, L19S10

Kok, J.F. and Renno, N.O. (2008), Electrostatics in wind-blown sand. Phys. Rev. Lett., 100, 014501

Kok, J. F., E. J. R. Parteli, T. I. Michaels, and D. Bou Karam (2012), The physics of wind-blown sand and dust, Reports on Progress in Physics, 75, 106901

Kok, J.F., S. Albani, N.M. Mahowald, and D.S. Ward (2014a), An improved dust emission model - Part 2: Evaluation in the Community Earth System Model, with implications for the use of dust source functions. *Atmospheric Chemistry and Physics* 14, 13043-13061.

Kok, J.F., N.M. Mahowald, G. Fratini, J.A. Gillies, M. Ishizuka, J.F. Leys, M. Mikami, M.S. Park, S.U. Park, R.S. Van Pelt, and T.M. Zobeck (2014b), An improved dust emission model - Part 1: Model description and comparison against measurements. *Atmospheric Chemistry and Physics*, 14, 13023-13041.

Kuepper, M., C. Duermann, C. de Beule, and G. Wurm (2014), Propulsion of Porous Plates in Thin Atmospheres by Temperature Fields, *Microgravity Science and Technology*, 25:311-318.

Küpper, M., and G. Wurm (2015), Thermal Creep Assisted Dust Lifting on Mars: Wind Tunnel Experiments for the Entrainment Threshold Velocity, *JGR-Planets*,120, 1346-1356.

Kurgansky, M. V., A. Montecinos, V. Villagran, and S. M. Metzger (2011), Micrometeorological conditions for dust-devil occurrence in the atacama desert, *Boundary-Layer Meteorol.*, 138 (2), 285-298, doi:10.1007/s10546-010-9549-1.

Lettau, K., and H. Lettau (1978), Experimental and micrometeorological field studies of dune migration., in Exploring the world's driest climate, edited by H. H. Lettau and K. Lettau, Madison, Center for Climatic Research, Univ. Wisconsin.

Loosmore, G. A., and J. R. Hunt (2000), Dust resuspension without saltation, J. Geophys. Res., 105 (D16), 20,663-20,671, doi:10.1029/2000JD900271.

Lorenz, R. D., L. D. Neakrase, and J. D. Anderson (2015), In-situ measurement of dust devil activity at La Jornada Experimental Range, New Mexico, USA , *Aeolian Research*, (0), doi: 10.1016/j.aeolia.2015.01.012.

Lorenz, R.D., and D. Reiss (2015), Solar panel clearing events, dust devil tracks and in-situ vortex detections on Mars, *Icarus* 248, 162-164, doi:10.1016/j.icarus.2014.10.034.

Lu, H., and Y. Shao (1999), A new model for dust emission by saltation bombardment, *J. Geophys. Res.*, 104, 16,827-16,842.

Macpherson, T., W. G. Nickling, J. A. Gillies, and V. Etyemezian (2008), Dust emissions from undisturbed and disturbed supply-limited desert surfaces, *Journal of Geophysical Research: Earth Surface*, 113 (F2), doi:10.1029/2007JF000800.

Mahowald, N., S. Albani, J.F. Kok, S. Engelstaeder, R. Scanza, D.S. Ward, and M.G. Flanner (2014), The size distribution of desert dust aerosols and its impact on the Earth system. *Aeolian Research* 15, 53-71.

Marticorena, B., and G. Bergametti (1995), Modeling the atmospheric dust cycle: 1. Design of a soil-derived dust emission scheme, *J. Geophys. Res.*, 100 (D8), 16,415-16,430.

Marticorena B., G. Bergametti, D. A. Gillette and J. Belnap (1997), Factors controlling threshold friction velocity in semi-arid and arid areas of the United States, *J. Geophys.Res*. ; 102, 23277-23287, 1997b.

McKenna Neuman, C. (2003), Effects of temperature and humidity upon the entrainment of sedimentary particles by wind, *Boundary-Layer Meteorol.*, 108, 61-89.

McKenna Neuman, C., and W. G. Nickling (1989), A theoretical and wind tunnel investigation of the effect of capillary water on the entrainment of sediment by wind, *Can. J. Soil Sci.*, 69, 79-96.

McKim, R.J. (1996), The dust storms of Mars, *J. Br. Astron. Assoc.*, 106, 185-200.

Merrison, J.P., Gunnlaugsson, H.P., Nørnberg, P., Jensen, A.E., Rasmussen, K.R. (2007), Determination of the Wind Induced Detachment Threshold for Granular Material on Mars using Wind Tunnel Simulations, *Icarus*, 191, 568-580.

Merrison, J.P. (2012), Sand Transport, Erosion and Granular Electrification, *Aeolian Research*, 4, 1–16.

Montabone, L., F. Forget, E. Millour, R.J. Wilson, S.R. Lewis, B. Cantor, D. Kass, A. Kleinböhl, M.T. Lemmon, M.D. Smith, and M.J.Wolff (2015), Eight-year climatology of dust optical depth on Mars, *Icarus*, 251, 65-95, doi:10.1016/j.icarus.2014.12.034.

Mulholland, D.P., A. Spiga, C. Listowski, and P.L. Read (2015), An assessment of the impact of local processes on dust lifting in martian climate models, *Icarus*, 252, 212-227, doi:10.1016/j.icarus.2015.01.017.

Muntz, E.P., Y. Sone, K. Aoki, S. Vargo, and M. Young (2002), *J. Vac. Sci. Technol*., A 20, 214.

Neakrase, L.D.V., R. Greeley, J.D. Iversen, M.R. Balme, and E.E. Eddlemon (2006), Dust flux within dust devils: Preliminary laboratory simulations, *Geophys. Res. Lett.*, 33, L19S09, doi:10.1029/2006GL026810.

Neakrase, L.D.V. and R. Greeley (2010a), Dust devil sediment flux on Earth and Mars: Laboratory simulations, *Icarus*, 206, 306-318, doi:10.1016/j.icarus.2009.08.028.

Neakrase, L.D.V. and R. Greeley (2010b), Dust devils in the laboratory: Effects of surface roughness on vortex dynamics, *J. Geophys. Res.*, 115, E05003, doi:10.1029/2009JE003465.

Newman, C.E., S.R. Lewis, P.L. Read, (2005). The atmospheric circulation and dust activity in different orbital epochs on Mars. *Icarus* 174, 135–160.

Newman, C.E., S.R. Lewis, P.L. Read, F. Forget (2002), Modeling the Martian dust cycle 1. Representationsof dust transport processes, *J. Geophys. Res.*, 107, E12, 5123, doi:10.1029/2002JE001910.

Oke, A. M. C., N. J. Tapper, and D. Dunkerley (2007), Willy-willies in the Australian landscape: The role of key meteorological variables and surface conditions in defining frequency and spatial characteristics, *J. Arid Environ*., 71, 201-215, doi:10.1016/j.jaridenv.2007.03.008.

Owen, R. P. (1964), Saltation of uniform grains in air, J. Fluid Mech., 20, 225-242.

Porch, W. M., and D. A. Gillette (1977), A Comparison of Aerosol and Momentum Mixing in Dust Storms Using Fast-Response Instruments, J. Appl. Meteorol., 16, 12, 1273-1281.

Prospero, J.M., P. Ginoux, O. Torres, S.E. Nicholson, and T.E. Gill (2002), Environmental characterization of global sources of atmospheric soil dust identified with the Nimbus 7 Total Ozone Mapping Spectrometer (TOMS) absorbing aerosol product. *Reviews of Geophysics* 40, 1002.

Raupach, M. (1992), Drag and drag partition on rough surfaces, *Boundary-Layer Meteorol.*, 60 (4),

375-395, doi:10.1007/BF00155203.

Raupach, M., J. Finnigan, and Y. Brunei (1996), Coherent eddies and turbulence in vegetation canopies: The mixing-layer analogy, *Boundary-Layer Meteorology*, 78 (3-4), 351-382, doi:10.1007/BF00120941.

Raupach, M. R., and H. Lu (2004), Representation of land-surface processes in aeolian transport models, *Environmental Modelling & Software*, 19 (2), 93-112, doi:10.1016/S1364-8152(03)00113-0, modelling of Wind Erosion and Aeolian Processes.

Raupach, M. R., D. A. Gilette, and J. F. Leys (1993), The effect of roughness elements on wind erosion threshold, *J. Geophys. Res*., 98 (D2), 3023{3029, doi:10.1029/92JD01922.

Reeks, M.W., D. Hall (2001), Kinetic models for particle resuspension in turbulent flows:theory and measurement, *J. Aerosol Sci.*, 32, 1–31.

Renno, N. O., Abreu, V. J., Koch, J., Smith, P. H., Hartogensis, o. K., De Bruin, H. A. R., Burose, D., Delory, G. T., Farrell, W. M., Watts, C. J., Garatuza, J., Parker, M., Carswell, A. (2004), MATADOR 2002: A pilot field experiment on convective plumes and dust devils. *J. Geophys. Res.,* Vol. 109, E07001, doi:10.1029/2003JE002219.

Ringrose, T.J., M.C. Towner, and J.C. Zarnecki (2003), Vortices on Mars: a reanalysis of Viking Lander 2 meterological data, sols 1-60, *Icarus*, 163, 78-87, doi:10.1016/S0019-1035(03)00073-3.

Rondeau, A., J. Merrison, J. J. Iversen, S. Peillona, J.-C. Sabroux, P. Lemaitre, F. Gensdarmes, E. Chassefièrec (2015), First experimental results of particle re-suspension in a low pressurewind tunnel applied to the issue of dust in fusion reactors, *Fusion Engineering and Design*, doi:10.1016/j.fusengdes.2014.12.038.

Roney, J. A., and B. R. White (2004), Definition and measurement of dust aeolian thresholds, *J. Geophys. Res.: Earth Surface*, 109 (F1), doi:10.1029/2003JF000061.

Rosenberg, P. D., et al. (2014), Quantifying particle size and turbulent scale dependence of dust flux in the Sahara using aircraft measurements, *J. Geophys. Res. Atmos*., 119, 7577–7598, doi:10.1002/2013JD021255.

Rudge, W.A.D. (1913), Atmospheric Electrification during South African Dust Storms. *Nature*, 91, 31.

Ryan, J.A., and R.D. Lucich (1983), Possible Dust Devils, Vortices on Mars, *J. Geophys. Res.*, 88, C15, 11,005-11,011.

Schlichting, H. (1936), Dusty ice clouds over Alaska, Ing.-Arch, 7, 1--34, *English translation: NACA Technical Memorandum*, No. 823-1936.

Schmidt, D. S., Schmidt, R. A., Dent, J. D. (1998), Electrostatic force on saltating sand. *J. Geophys. Res.,* Vol. 103, No. D8, 8997-9001.

Shao, Y. (2001), A model for mineral dust emission, *J. Geophys. Res.*, 106 (D17), 20,239-20,254.

Shao, Y. (2004), Simplification of a dust emission scheme and comparison with data, *J. Geophys. Res.*, 109, D10202, doi:10.1029/2003JD004372.

Shao, Y. (2008), Physics and Modelling of Wind Erosion, 2 ed., 452 pp., Springer-Verlag, Berlin.

Shao, Y., and H. Lu (2000), A simple expression for wind erosion threshold friction velocity, *J. Geophys. Res.*, 105, 22,437-22,443.

Shao, Y., and Y. Yang (2008), A theory for drag partition over rough surfaces, *J. Geophys. Res.,* 113, F02S05, doi:10.1029/2007JF000791.

Shao, Y., M. R. Raupach, and P. A. Findlater (1993), The effect of saltation bombardment on the entrainment of dust by wind, *J. Geophys. Res.,* 98, 12,719-12,726.

Shao, Y., M. R. Raupach, and J. F. Leys (1996), A model for predicting aeolian sand drift and dust entrainment on scales from paddock to region, Aust. J. Soil Res., 34, 309-342.

Shao, Y., A. H. Fink, and M. Klose (2010), Numerical simulation of a continental-scale Saharan dust event, *J. Geophys. Res.*, 115, D13205, doi:10.1029/2009JD012678.

Shao, Y., K.-H. Wyrwoll, A. Chappell, J. Huang, Z. Lin, G. H. McTainsh, M. Mikami, T. Y. Tanaka, X. Wang, and S. Yoon (2011), Dust cycle: An emerging core theme in Earth system science, *Aeolian Research*, 2, 181-204, doi:10.1016/j.aeolia.2011.02.001.

Shao, Y., M. Ishizuka, M. Mikami, and J. F. Leys (2001), Parameterization of size-resolved dust emission and validation with measurements, J. Geophys. Res., 116, D08203, doi:10.1029/2010JD014527.

Sinclair, P. C. (1969), General characteristics of dust devils, *J. Appl. Meteor.*, 8, 32-45, doi: 10.1175/1520-0450(1969)008h0032:GCODDi2.0.CO;2.

Smits, A.J., B.J. McKeon, and I. Marusic (2011), High-Reynolds Number Wall Turbulence. *Annual Review of Fluid Mechanics*, Vol 43 43, 353-375.

Snow, J. T., and T. M. McClelland (1990), Dust devils at White Sands Missile Range, New Mexico: 1. Temporal and spatial distributions, *J. Geophys. Res. Atmos.*, 95 (D9), 13,707-13,721, doi: 10.1029/JD095iD09p13707.

Sone, Y. & Itakura, E. (1990), *J. Vac. Soc. Jpn.*, 33, 92

Sow M., S. C. Alfaro, J. L. Rajot and B. Marticorena (2009), Size resolved dust emission fluxes measured in Niger during 3 dust storms of the AMMA experiment, Atmos. Chem. Phys., 9, 12, 3881-3891.

Stempniewicz, M.M., E.M.J. Komen, A. de With (2008), Model of particle resuspension inturbulent flow, *Nucl. Eng. Des.,* 328, 2943–2959.

Stout, J. E., and T. M. Zobeck (1997), Intermittent saltation, *Sedimentology*, 44, 959-970.

Stull, R. B. (1988), An Introduction to Boundary Layer Meteorology, 666 pp., Kluwer Academic Publishers, Norwell.

Stow, C. D. (1969), Dust and sand storm electrification, *Weather*, 24134-24137.

Sullivan, R., Banfield, D., Bell III, J.F., Calvin, W., Fike, D., Golombek, M., Greeley, R., Grotzinger, J., Herkenhoff, K., Jerolmack, D., Malin, M., Ming, D., Soderblom, L.A., Squyres, S.W., Thompson, S., Watters, W.A., Weitz, C.M., Yen, A. (2005). Aeolian processes at the Mars exploration rover Meridiani Planum landing site, *Nature* 436, 58–61.

Sullivan, R., R. Arvidson, J.F. Bell III, R. Gellert, M. Golombek, R. Greeley, K. Herkenhoff, J. Johnson, S. Thompson, P. Whelley, and J. Wray (2008), Wind-driven particle mobility on Mars: Insights from Mars Exploration Rover observations at 'El Dorado' and surroundings at Gusev Crater, *J. Geophys. Res.,* 113, E06S07, doi:10.1029/2008JE003101.

Towner, M.C., M.R. Patel, T.J. Ringrose, J.C. Zarnecki, D. Pullan, M.R. Sims, S. Haapanala, A.-M. Harri, J. Polkko, C.F. Wilson, R.C. Quinn, F.J. Grunthaner, M.H. Hecht, and J.R.C. Garry (2004), The Beagle 2 environmental sensors : science goals and instrument description, *Planetary and Space Science*, 52, 13, 1141-1156, doi :10.1016/j.pss.2004.07.015.

Wieringa, J. (1993), Representative roughness parameters for homogeneous terrains, *Boundary Layer Meteorol*., 63, 323–363.

Williams, E., Nathou, N., Hicks, E., Pontikis, C., Russel, B., Miller, M., Bartholomew, M.J. (2009), The electrification of dust-lofting gust fronts ('haboobs') in the Sahel. *Atm. Res.*, 91, 292-298.

Wolff, M.J., M.D. Smith, R.T. Clancy, N. Spanovich, B.A. Whitney, M.T. Lemmon, J.L.Bandfield, D. Bandfield, A. Ghosh, G. Landis, P.R. Christensen, J.F. Bell III, and S.W. Squyres, Constraints on dust aerosols from the Mars Exploration Rovers using MGS overflights and Mini-TES, *J. Geophys. Res.*, 111, E12S17, doi:10.1029/2006JE002786.

Wurm, G. and O. Krauss (2006), Dust Eruptions by Photophoresis and Solid State Greenhouse Effects, *Physical Review Letters*, 96:134301 1-4.

Wurm, G. and O. Krauss (2008), Experiments on Negative Photophoresis and Application to the Atmosphere, *Atmospheric Environment*, 42:2682-2690.

Wurm, G., J. Teiser, and D. Reiss (2008), Greenhouse and Thermophoretic Effects in Dust Layers: The Missing Link for Lifting Dust on Mars, *Geophysical Research Letters*, 35:L10201 1-5.

Ungar, J.E., and P.K. Haff (1987), Steady-state saltation in air. *Sedimentology* 34, 289-299.

Vargo, S. E., E. P. Muntz, G. R. Shiflett, and W. C. Tang (1999) *J. Vac. Sci. Technol.* A 17, 2308.

Yizhaq, H. J. F. Kok, and I. Katra (2014), Basaltic sand ripples at Eagle crater as indirect evidence for the hysteresis effect in martian saltation, *Icarus*, 230, 143-50.

Zheng, X. J., Huang, N. & Zhou, Y. H. (2003), Laboratory measurement of electrification of wind-blown sands and simulation of its effect on sand saltation movement. *J. Geophys. Res.* 108, 4322.

Zimon, A. D. (1982), Adhesion of dust and powder, 438 pp., Consultants Bureau, New York.

Ziskind, G., Fichman, M., and Gutfinger, C. (1995), Resuspension of particulates from surfaces to turbulent flows – review and analysis, *J. Aerosol Sci*., 26, 613-644.

Zurek, R.W., and L.J. Martin (1993), Interannual variability of planet-encircling dust activity on Mars, *J. Geophys. Res.*, 98, 3247-3259.